BULLETIN OF THE EARTHQUAKE
RESEARCH INSTITUTE
Vol. 43 (1965), pp. 459-498

31. *A Long Wave in the Vicinity of an Estuary [II] —An Analysis by the Method of the Buffer Domain—.*

By Takao MOMOI,

Earthquake Research Institute.

(Read June 22, 1965.—Received June 30, 1965.)

Abstract

Succeeding the previous study on long waves in the vicinity of an estuary, the theory is developed, in this paper, under the second approximation to inquire numerically into the behaviors of the waves around an estuary. When the approximation proceeds from the first to the second one, the minute behaviors of the waves come to light, which do not appear in the first approximation. The newly exposed facts are as follows:—

High waves appear in the interior of the canal, which is due to the diffraction of the waves in the estuary.

The way in which the incident waves invade the canal is such that the waves first advance towards the center of the mouth of the canal from the open sea (of which the crest line is a triangular form) and then, as they progress, they are diverted to the direction of the axis of the canal.

The damping reflected waves in the open sea are not so much affected, when the approximation is generalized from the first to the second one, expecting that the directivity of the damping reflected waves is smoothed.

In developing the theory, a basic principle is based on the method of the buffer domain which has been introduced by the author.

1. Introduction

In the previous paper[1] (referred to as paper I in the following discussion), a long wave in the vicinity of an estuary was studied under the first order of the approximation. Then a new method named as "the method of the buffer domain" was used, which was first introduced by the author.[2] In the present purview, the theory is developed under the second order of the approximation and further discussions are made for

1) T. MOMOI, *Bull. Earthq. Res. Inst.*, **43** (1965), 291.
2) T. MOMOI, *Bull. Earthq. Res. Inst.*, **43** (1965), 289.

the waves around an estuary.

The definitions and notations used in this paper are outlined in section 2, which are completely the same as those in paper I, unless otherwise stated.

Since the general theory without any simplification has already been described in paper I, the derivation of the general theory is not given in the present purview. For the general theory, if necessary, readers should refer to the previous study[1].

2. Definitions and Notations

In this section, the definitions and notations used in this paper are summarized (refer to Fig. 1).

x, y : the Cartesian coordinates;
r, θ : the polar coordinates;
t : a variable of time;
c : a velocity of a long wave;
D_j $(j=1, 2, 3)$: the domains in the ranges $(|x|<d, y<0)$, $(r<d, 0<\theta<\pi)$ and $(r>d, 0<\theta<\pi)$;
k : a wave number of an incident wave;
ω : an angular frequency of an incident wave;
ζ_j $(j=1, 2, 3)$: wave heights in the domains D_j;

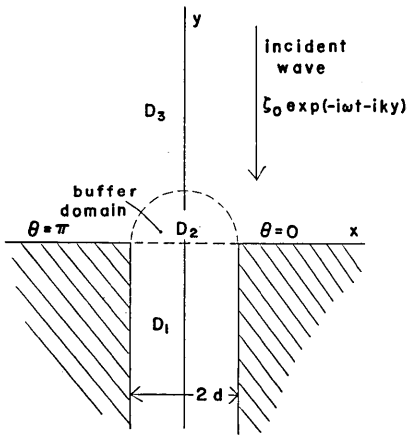

Fig. 1. A geometry of a used model.

ζ_0 : an amplitude of invading waves;
d : half a width of a canal;
$\zeta_1^{(m)}$ $(m=0, 1, 2, \cdots)$: the amplitude factor of the m-th mode of the waves in the domain D_1 or the canal;
$\overline{\zeta}_2^{(2n)}, \zeta_2^{(2n+1)}$ $(n=0, 1, 2, \cdots)$: the amplitude factors for the $2n$-th cosine and $(2n+1)$-th sine modes of the waves in the domain D_2;
$\zeta_3^{(2m)}$ $(m=0, 1, 2, \cdots)$: the amplitude factor of the $2m$-th cosine mode of the waves in the domain D_3 or the open sea.

3. Outline of General Theory

In this section, the general theory developed in paper I is outlined. An entire portion of the analysis is based on a long wave equation, i.e., (by use of the Cartesian coordinates)

$$\frac{\partial^2\zeta}{\partial x^2}+\frac{\partial^2\zeta}{\partial y^2}=\frac{1}{c^2}\cdot\frac{\partial^2\zeta}{\partial t^2}\,; \tag{1}$$

(by use of the polar coordinates)

$$\frac{\partial^2\zeta}{\partial r^2}+\frac{1}{r}\cdot\frac{\partial\zeta}{\partial r}+\frac{1}{r^2}\cdot\frac{\partial^2\zeta}{\partial\theta^2}=\frac{1}{c^2}\cdot\frac{\partial^2\zeta}{\partial t^2}\,. \tag{2}$$

Boundary conditions are such that there exist no fluxes at the rigid boundaries, i.e.,

$$\frac{\partial\zeta}{\partial n}=0 \tag{3}$$

where $\partial/\partial n$ is a derivative in the direction perpendicular to the rigid boundaries.

The equation (1) or (2) can be solved formally so as to satisfy the boundary condition (3) in each domain $D_j\,(j=1, 2, 3)$. The formal solutions obtained involve the unknowns as coefficients. For these formal solutions, reference should be made to paper I.

In order to obtain the explicit expressions of the unknowns, other conditions are required, which are provided by the conditions :— the continuity of wave height

$$\zeta_a=\zeta_b\,,$$

the continuity of flux

$$\frac{\partial\zeta_a}{\partial s}=\frac{\partial\zeta_b}{\partial s}\,, \tag{4}$$

where ζ_a and ζ_b are the wave heights in the neighbouring domains, and $\partial/\partial s$ a derivative orthogonal to the boundary between the adjacent domains.

Substituting the formal solutions into (4) and applying appropriate operators to these relations, we have the following simultaneous equations (refer to paper I) :—

$$\sum_{n=0}^{\infty} I(J_{2n},\, m)\cdot\bar{\zeta}_2^{(2n)}-\varepsilon_m\cdot kd\cdot\zeta_1^{(m)}=0\,, \tag{5}$$

$$\sum_{n=0}^{\infty} I\left(\frac{J_{2n+1}}{r},\, m\right)\cdot\zeta_2^{(2n+1)}+i\cdot\varepsilon_m\cdot k_1^{(m)}d\cdot\zeta_1^{(m)}=0\,, \tag{6}$$

$$J_{2m}(kd)\cdot\bar{\zeta}_2^{(2m)}+\frac{1}{\varepsilon_m}\cdot\sum_{n=0}^{\infty}\frac{2}{\pi}\cdot\frac{(2n+1)\cdot J_{2n+1}(kd)}{(2n+1)^2-(2m)^2}\cdot\zeta_2^{(2n+1)}$$
$$=H_{2m}^{(1)}(kd)\cdot\zeta_3^{(2m)}+\frac{1}{\varepsilon_m}\cdot 2J_{2m}(kd)\cdot\zeta_0\,, \tag{7}$$

$$J'_{2m}(kd)\cdot\bar{\zeta}_2^{(2m)}+\frac{1}{\varepsilon_m}\sum_{n=0}^{\infty}\frac{2}{\pi}\cdot\frac{(2n+1)\cdot J'_{2n+1}(kd)}{(2n+1)^2-(2m)^2}\cdot\zeta_2^{(2n+1)}$$
$$=H_{2m}^{(1)\prime}(kd)\cdot\zeta_3^{(2m)}+\frac{1}{\varepsilon_m}\cdot 2J'_{2m}(kd)\cdot\zeta_0\,, \tag{8}$$

where m is a non-negative integer;

$$\varepsilon_m=\begin{cases}1 & (m=0)\,,\\ \dfrac{1}{2} & (m\geqq 1)\,;\end{cases}$$

and

$$\left.\begin{aligned} I(J_{2n},\,q)&=\int_0^{kd}J_{2n}(z)\cos\frac{q\pi}{kd}z\,dz\,,\\ I\Big(\frac{J_{2n+1}}{r},\,q\Big)&=(2n+1)\int_0^{kd}\frac{J_{2n+1}(z)}{z}\cos\frac{q\pi}{kd}z\,dz\,,\\ &(n,\,q=0,\,1,\,2,\,\cdots)\,.\end{aligned}\right\} \tag{9}$$

Since the equations (5)–(8) are infinite simultaneous equations, they must be solved as a finite number of simultaneous equations. For this purpose, the method of the buffer domain is available.[3] Using this method, a further reduction is made in the subsequent section.

4. Second Approximation

In paper I, the domain D_2 is considered as the buffer domain, to which the approximation:

$$\left.\begin{aligned} J_0(z)&\simeq 1\,,\\ J_1(z)&\simeq\frac{z}{2}\,,\\ J_m(z)&\simeq 0 \qquad (m\geqq 2)\,,\end{aligned}\right\} \tag{10}$$

is given.

In the present work, the more generalized approximation:

3) T. MOMOI, *loc. cit.*, 2).

$$\left.\begin{aligned} J_0(z) &\simeq 1-\left(\frac{z}{2}\right)^2, \\ J_1(z) &\simeq \frac{z}{2}\,. \\ J_2(z) &\simeq \frac{1}{2}\left(\frac{z}{2}\right)^2, \\ J_m(z) &\simeq 0 \qquad (m\geqq 3)\,, \end{aligned}\right\} \tag{11}$$

is employed in the reduction of the equations.

The approximation (11) denotes that the Bessel functions are retained up to the terms of the second order of $(z/2)$, while, in (10), a linear approximation is given to the power series of the Bessel functions.

Substituting (11) into (9) and after a few reductions, we have :—

$$I(J_0, q)\begin{cases} = kd-\dfrac{1}{12}(kd)^3 & (q=0)\,, \\ = (-1)^{q+1}\cdot\dfrac{1}{2(q\pi)^2}\cdot(kd)^3 & (q\geqq 1)\,, \end{cases} \tag{12}$$

$$I(J_2, q)\begin{cases} = \dfrac{1}{24}\cdot(kd)^3 & (q=0)\,, \\ = (-1)^{q}\cdot\dfrac{1}{4(q\pi)^2}\cdot(kd)^3 & (q\geqq 1)\,, \end{cases} \tag{13}$$

$$I(J_{2n}, q)=0 \qquad (n\geqq 2,\ q=0, 1, 2, \cdots)\,, \tag{14}$$

$$I\left(\frac{J_1}{r}, q\right)\begin{cases} = \dfrac{1}{2}kd & (q=0)\,, \\ = 0 & (q\geqq 1)\,, \end{cases} \tag{15}$$

$$I\left(\frac{J_{2n+1}}{r}, q\right)=0 \qquad (n\geqq 1,\ q=0, 1, 2, \cdots)\,. \tag{16}$$

From (11), the derivatives of the Bessel functions are as follows :—

$$\left.\begin{aligned} J_0'(z) &\simeq -\frac{z}{2}\,, \\ J_1'(z) &\simeq \frac{1}{2}\,, \\ J_2'(z) &\simeq \frac{z}{4}\,, \\ J_m(z) &\simeq 0 \qquad (m\geqq 3)\,. \end{aligned}\right\} \tag{17}$$

Since we are using the method of the buffer domain, the approximation must be applied merely to the buffer domain, i.e. domain D_2. Therefore, applying the aforementioned approximations (12)–(17) to the expressions relevant to the buffer domain D_2, we have the following equations :—

$$\left.\begin{aligned} I(J_0, 0)\cdot\bar{\zeta}_2^{(0)}+I(J_2, 0)\cdot\bar{\zeta}_2^{(2)}-kd\cdot\zeta_1^{(0)}&=0\ ,\\ I(J_0, m)\cdot\bar{\zeta}_2^{(0)}+I(J_2, m)\cdot\bar{\zeta}_2^{(2)}-\frac{kd}{2}\cdot\zeta_1^{(m)}&=0\\ (m=1, 2, 3, \cdots)\ ,& \end{aligned}\right\} \tag{18}$$

$$\left.\begin{aligned} I\left(\frac{J_1}{r}, 0\right)\cdot\zeta_2^{(1)}+ikd\cdot\zeta_1^{(0)}&=0\ ,\\ i\cdot\frac{1}{2}k_1^{(m)}d\cdot\zeta_1^{(m)}&=0\\ (m=1, 2, 3, \cdots)\ ,& \end{aligned}\right\} \tag{19}$$

$$\left.\begin{aligned} &J_0(kd)\cdot\bar{\zeta}_2^{(0)}+\frac{2}{\pi}J_1(kd)\cdot\zeta_2^{(1)}\\ &\quad=H_0^{(1)}(kd)\cdot\zeta_3^{(0)}+2J_0(kd)\cdot\zeta_0\ ,\\ &J_2(kd)\cdot\bar{\zeta}_2^{(2)}+\frac{4}{\pi}\cdot\frac{1}{-3}\cdot J_1(kd)\cdot\zeta_2^{(1)}\\ &\quad=H_2^{(1)}(kd)\cdot\zeta_3^{(2)}+4J_2(kd)\cdot\zeta_0\ ,\\ &\frac{4}{\pi}\cdot\frac{1}{1-(2m)^2}\cdot J_1(kd)\cdot\zeta_2^{(1)}\\ &\quad=H_{2m}^{(1)}(kd)\cdot\zeta_3^{(2m)}+4J_{2m}(kd)\cdot\zeta_0\\ &\qquad(m=2, 3, 4, \cdots)\ , \end{aligned}\right\} \tag{20}$$

$$\left.\begin{aligned} &J_0'(kd)\cdot\bar{\zeta}_2^{(0)}+\frac{2}{\pi}J_1'(kd)\cdot\zeta_2^{(1)}\\ &\quad=H_0^{(1)\prime}(kd)\cdot\zeta_3^{(0)}+2J_0'(kd)\cdot\zeta_0\ ,\\ &J_2'(kd)\cdot\bar{\zeta}_2^{(2)}+\frac{4}{\pi}\frac{1}{-3}\cdot J_1'(kd)\\ &\quad=H_2^{(1)\prime}(kd)\cdot\zeta_3^{(2)}+4J_2'(kd)\cdot\zeta_0\ ,\\ &\frac{4}{\pi}\cdot\frac{1}{1-(2m)^2}\cdot J_1'(kd)\cdot\zeta_2^{(1)}\\ &\quad=H_{2m}^{(1)\prime}(kd)\cdot\zeta_3^{(2m)}+4J_{2m}'(kd)\cdot\zeta_0\\ &\qquad(m=2, 3, 4, \cdots)\ , \end{aligned}\right\} \tag{21}$$

where

$$\left.\begin{matrix} I(J_0, q)\ , \\ I(J_2, q)\ , \end{matrix}\right\} \quad (q=0, 1, 2, \cdots)\ , \qquad I\left(\frac{J_1}{r}, 0\right)\ ,$$

$J_0(kd)$, $J_1(kd)$, $J_2(kd)$, $J_0'(kd)$, $J_1'(kd)$, and $J_2'(kd)$

are expressed in (12)–(17).

Using the first relation of (18) and the second equation for $m=1$ in (18), $\overline{\zeta}_2^{(0)}$ and $\overline{\zeta}_2^{(2)}$ are expressed explicitly by $\zeta_1^{(0)}$ and $\zeta_1^{(1)}$, i.e.,

$$\left.\begin{aligned} \overline{\zeta}_2^{(0)} &= \frac{1}{\Delta}\cdot\left\{kd\cdot I(J_2, 1)\cdot\zeta_1^{(0)} - \frac{kd}{2}\cdot I(J_2, 0)\cdot\zeta_1^{(1)}\right\}, \\ \overline{\zeta}_2^{(2)} &= \frac{1}{\Delta}\cdot\left\{\frac{kd}{2}\cdot I(J_0, 0)\cdot\zeta_1^{(1)} - kd\cdot I(J_0, 1)\cdot\zeta_1^{(0)}\right\}, \end{aligned}\right\} \tag{22}$$

where

$$\Delta = I(J_0, 0)\cdot I(J_2, 1) - I(J_0, 1)\cdot I(J_2, 0)\ . \tag{23}$$

By use of (15), the first relation of (19) becomes

$$\zeta_2^{(1)} = -i\cdot 2\zeta_1^{(0)}\ . \tag{24}$$

Substituting the first expression of (22) and (24) into the first equation of (20), we have

$$\begin{aligned} &\frac{J_0(kd)}{\Delta}\cdot\left\{kd\cdot I(J_2, 1)\cdot\zeta_1^{(0)} - \frac{kd}{2}\cdot I(J_2, 0)\cdot\zeta_1^{(1)}\right\} - i\cdot\frac{4}{\pi}\cdot J_1(kd)\cdot\zeta_1^{(0)} \\ &\qquad = H_0^{(1)}(kd)\cdot\zeta_3^{(0)} + 2J_0(kd)\cdot\zeta_0\ . \end{aligned} \tag{25}$$

Likewise, substituting the second expression of (22) and (24) into the second equation of (20), we have

$$\begin{aligned} &\frac{J_2(kd)}{\Delta}\cdot\left\{\frac{kd}{2}\cdot I(J_0, 0)\cdot\zeta_1^{(1)} - kd\cdot I(J_0, 1)\cdot\zeta_1^{(0)}\right\} + i\cdot\frac{8}{3\pi}\cdot J_1(kd)\cdot\zeta_1^{(0)} \\ &\qquad = H_2^{(1)}(kd)\cdot\zeta_3^{(2)} + 4J_2(kd)\cdot\zeta_0\ . \end{aligned} \tag{26}$$

Putting the first expression of (22) and (24) into the first equation of (21), (21) becomes

$$\begin{aligned} &\frac{J_0'(kd)}{\Delta}\cdot\left\{kd\cdot I(J_2, 1)\cdot\zeta_1^{(0)} - \frac{kd}{2}\cdot I(J_2, 0)\cdot\zeta_1^{(1)}\right\} - i\cdot\frac{4}{\pi}\cdot J_1'(kd)\cdot\zeta_1^{(0)} \\ &\qquad = H_0^{(1)\prime}(kd)\cdot\zeta_3^{(0)} + 2J_0'(kd)\cdot\zeta_0\ . \end{aligned} \tag{27}$$

Likewise, a substitution of the second expression of (22) and (24) into the second equation of (21) yields

$$\frac{J_2'(kd)}{\Delta}\cdot\left\{\frac{kd}{2}\cdot I(J_0,0)\cdot\zeta_1^{(1)}-kd\cdot I(J_0,1)\cdot\zeta_1^{(0)}\right\}+i\cdot\frac{8}{3\pi}\cdot J_1'(kd)\cdot\zeta_1^{(0)}$$
$$=H_2^{(1)\prime}(kd)\cdot\zeta_3^{(2)}+4J_2'(kd)\cdot\zeta_0\,. \tag{28}$$

Eliminating $\zeta_3^{(0)}$ from (25) and (27) and after some reduction, we have

$$\frac{1}{\Delta}\cdot\left\{kd\cdot I(J_2,1)\cdot\zeta_1^{(0)}-\frac{kd}{2}\cdot I(J_2,0)\cdot\zeta_1^{(1)}\right\}$$
$$-2kd\cdot\{J_1(kd)\cdot H_0^{(1)\prime}(kd)-J_1'(kd)\cdot H_0^{(1)}(kd)\}\cdot\zeta_1^{(0)}=2\zeta_0\,. \tag{29}$$

where Lommel's relation

$$J_n(kd)\cdot H_n^{(1)\prime}(kd)-J_n'(kd)\cdot H_n^{(1)}(kd)=i\cdot\frac{2}{\pi kd}$$

is used.

Likewise, the elimination of $\zeta_3^{(2)}$ from (26) and (28) yields

$$\frac{1}{\Delta}\cdot\left\{\frac{kd}{2}\cdot I(J_0,0)\cdot\zeta_1^{(1)}-kd\cdot I(J_0,1)\cdot\zeta_1^{(0)}\right\}$$
$$+\frac{4}{3}kd\cdot\{J_1(kd)\cdot H_2^{(1)\prime}(kd)-J_1'(kd)\cdot H_2^{(1)}(kd)\}\cdot\zeta_1^{(0)}=4\zeta_0\,. \tag{30}$$

From (29) and (30), a further elimination of $\zeta_1^{(1)}$ yields, after a few reductions,

$$\zeta_1^{(0)}=\frac{2\zeta_0\cdot\{I(J_0,0)+2I(J_2,0)\}}{kd\cdot\left(1-2\cdot P_0+\frac{4}{3}\cdot P_2\right)}, \tag{31}$$

where

$$P_j=I(J_j,0)\cdot\{J_1(kd)\cdot H_j^{(1)\prime}(kd)-J_1'(kd)\cdot H_j^{(1)}(kd)\} \tag{31'}$$
$$(j=0,2)\,.$$

Using the approximate expressions (11)–(17), the above expression becomes

$$\zeta_1^{(0)}=\frac{2\zeta_0}{Q_1}, \tag{32}$$

where

$$\left.\begin{aligned} ReQ_1 &= 1+kd+\frac{1}{6}(kd)^3-\frac{5}{288}(kd)^5 , \\ ImQ_1 &= \left\{kd-\frac{(kd)^3}{12}\right\}\cdot\{Y_0(kd)+kd\cdot Y_1(kd)\} \\ &\quad +\frac{(kd)^3}{36}\cdot\{Y_2(kd)-kd\cdot Y_3(kd)\} , \end{aligned}\right\} \tag{33}$$

and where the recurrence formula of the Bessel function for the derivative of $Y_n(kd)$ has been used in the above reduction.

Multiplying (29) by $I(J_0, 1)$ and (30) by $I(J_2, 1)$, and adding two equations, we have

$$\frac{kd}{2}\cdot\zeta_1^{(1)}=\left(2kd\cdot R_0-\frac{4}{3}kd\cdot R_2\right)\cdot\zeta_1^{(0)}+2\{I(J_0, 1)+2I(J_2, 1)\}\cdot\zeta_0 , \tag{34}$$

where

$$R_j=I(J_j, 1)\cdot\{J_1(kd)\cdot H_j^{(1)\prime}(kd)-J_1'(kd)\cdot H_j^{(1)}(kd)\} \tag{34'}$$
$$(j=0, 2) .$$

Substituting (32) into (34) and after some reductions, (34) becomes

$$\begin{aligned} \zeta_1^{(1)}=\frac{4\zeta_0}{kd\cdot Q_1}\cdot\Big[&\{I(J_0, 1)+2I(J_2, 1)\} \\ &+\{2kd\cdot I(J_0, 1)-2I(J_0, 0)\cdot I(J_0, 1)-4I(J_0, 0)\cdot I(J_2, 1)\}\cdot S_0 \\ &+\left\{-\frac{4}{3}kd\cdot I(J_2, 1)+\frac{4}{3}I(J_2, 0)\cdot I(J_0, 1)+\frac{8}{3}I(J_2, 0)\cdot I(J_2, 1)\right\}\cdot S_2\Big], \end{aligned} \tag{35}$$

where

$$S_j=J_1(kd)\cdot H_j^{(1)\prime}(kd)-J_1'(kd)\cdot H_j^{(1)}(kd) . \tag{35'}$$

By use of (11)–(17) and the relation of the Bessel function

$$Y_n'(kd)=\frac{n}{kd}\cdot Y_n(kd)-Y_{n+1}(kd) ,$$

the expression (35) is reduced to

$$\zeta_1^{(1)}=2\cdot\frac{(kd)^3}{\pi^2}\cdot\frac{Q_2}{Q_1}\cdot\zeta_0 \tag{36}$$

where

$$\left.\begin{aligned} ReQ_2 &= -\left\{1+\frac{5}{6}\left(\frac{kd}{2}\right)^2\right\}, \\ ImQ_2 &= -\{Y_0(kd)+kd\cdot Y_1(kd)\} \\ &\quad +\frac{1}{3}\{Y_2(kd)-kd\cdot Y_3(kd)\}, \end{aligned}\right\} \tag{37}$$

and Q_1 is given in (33).

Next, let us obtain the expression for $\zeta_3^{(0)}$.

Multiplying (25) by $J_0'(kd)$ and (27) by $J_0(kd)$, and subtracting the latter from the former, the expression

$$\zeta_3^{(0)}=2kd\cdot\{J_1(kd)J_0'(kd)-J_1'(kd)J_0(kd)\}\cdot\zeta_1^{(0)} \tag{38}$$

is obtained, where Lommel's relation for the Bessel function is employed in this reduction.

Substituting the approximate expressions of the Bessel functions (11) and the derivatives of the Bessel functions (17) into (38), we have

$$\zeta_3^{(0)}=-kd\cdot\left\{1+\left(\frac{kd}{2}\right)^2\right\}\cdot\zeta_1^{(0)}. \tag{39}$$

Likewise, multiplying (26) by $J_2'(kd)$ and (28) by $J_2(kd)$, and subtracting the latter from the former, the expression for $\zeta_3^{(2)}$ becomes

$$\zeta_3^{(2)}=-\frac{4}{3}kd\cdot\{J_1(kd)J_2'(kd)-J_1'(kd)J_2(kd)\}\cdot\zeta_1^{(0)},$$

where Lommel's formula of the Bessel function is used.

Putting (11) and (17) into the above expression, we have

$$\zeta_3^{(2)}=-\frac{1}{3}kd\cdot\left(\frac{kd}{2}\right)^2\cdot\zeta_1^{(0)}. \tag{40}$$

Now, Substituting (32) into (39) and (40), these expressions become

$$\left.\begin{aligned} \zeta_3^{(0)} &= -\frac{2}{Q_1}\cdot kd\cdot\left\{1+\left(\frac{kd}{2}\right)^2\right\}\cdot\zeta_0, \\ \zeta_3^{(2)} &= -\frac{1}{6}\cdot\frac{1}{Q_1}\cdot(kd)^3\cdot\zeta_0. \end{aligned}\right\} \tag{41}$$

From the last equation of (20), the approximate expressions of the Bessel functions and (24), the higher modes of the waves ($m\geqq 2$) in the

domain D_3 are expressed as

$$\zeta_3^{(2m)}=\frac{4}{\pi}\cdot\frac{1}{(2m)^2-1}\cdot\frac{kd}{Y_{2m}(kd)}\cdot\zeta_1^{(0)}\ . \tag{42}$$

Using (32), the above expression is further reduced to

$$\zeta_3^{(2m)}=\frac{8}{\pi}\cdot\frac{kd}{Q_1}\cdot\frac{1}{(2m)^2-1}\cdot\frac{1}{Y_{2m}(kd)}\cdot\zeta_0 \qquad (m\geqq 2)\ . \tag{43}$$

Thus, each mode of the waves in the domain D_3 (in the open sea) is given by (41) and (43). Then the wave height in the open sea is expressed (refer to paper I) by the series

$$\zeta_3=2\zeta_0\cdot\cos ky+\zeta_{re}^{(\mathrm{damp})}\ , \tag{44}$$

where

$$\zeta_{re}^{(\mathrm{damp})}=\sum_{m=0}^{\infty}\zeta_3^{(2m)}\cdot H_{2m}^{(1)}(kr)\cdot\cos 2m\theta\ . \tag{45}$$

Here, the second term of (44), i.e., (45) denotes the damping waves reflected from the estuary of the canal.

Next, let us obtain the expression of the wave height in the domain D_2.

From (24) and (32), the first mode of the wave in the domain D_2 becomes

$$\zeta_2^{(1)}=-i\cdot\frac{4}{Q_1}\cdot\zeta_0\ . \tag{46}$$

Eliminating $\zeta_2^{(1)}$ and $\zeta_3^{(0)}$ from the first equation of (20), (41) and (46), we have

$$\overline{\zeta}_2^{(0)}=2\cdot\left\{1+kd\cdot\frac{Q_3}{Q_1}\right\}\cdot\zeta_0\ , \tag{47}$$

where

$$\left.\begin{aligned} ReQ_3&=-\left\{1+\left(\frac{kd}{2}\right)^2\right\}\ ,\\ ImQ_3&=\frac{1}{1-\left(\frac{kd}{2}\right)^2}\cdot\left[\frac{2}{\pi}-\left\{1+\left(\frac{kd}{2}\right)^2\right\}\cdot Y_0(kd)\right]\ , \end{aligned}\right\} \tag{48}$$

and the approximated expression of the Bessel function is used.

Likewise, eliminating $\zeta_2^{(1)}$ and $\zeta_3^{(2)}$ from the second relation of (20), the second expression of (41) and (46), we have

$$\bar{\zeta}_2^{(2)}=2\cdot\left\{2+kd\cdot\frac{Q_4}{Q_1}\right\}\cdot\zeta_0\ , \tag{49}$$

where

$$\left.\begin{aligned} ReQ_4&=-\frac{1}{3}\left(\frac{kd}{2}\right)^2\ ,\\ ImQ_4&=-\frac{8}{(kd)^2}\cdot\left\{\frac{4}{3\pi}+\frac{1}{3}\left(\frac{kd}{2}\right)^2\cdot Y_2(kd)\right\}\ , \end{aligned}\right\} \tag{50}$$

and the approximate forms of the Bessel functions are used in the above reduction.

Though the waves in the domain D_2 are described (refer to paper I) as

$$\zeta_2=\sum_{m=0}^{\infty}\{\bar{\zeta}_2^{(2m)}\cos 2m\theta\cdot J_{2m}(kr)+\zeta_2^{(2m+1)}\sin(2m+1)\theta\cdot J_{2m+1}(kr)\}\ ,$$

the above expression is reduced, in the approximation used in this purview, to the form :—

$$\zeta_2=\bar{\zeta}_2^{(0)}J_0(kr)+\zeta_2^{(1)}\sin\theta\cdot J_1(kr)+\bar{\zeta}_2^{(2)}\cos 2\theta\cdot J_2(kr)\ . \tag{51}$$

Now, the behaviors of the waves in the domain D_2 are expressed, in the approximation of the second order of kd, by (46), (47), (49) and (51).

Finally, let us obtain the solution in the domain D_1.

Substituting (12) and (13) into the second relation of (18), the higher modes of the waves in the canal are expressed as

$$\zeta_1^{(m)}=(-1)^m\cdot\left(\frac{kd}{m\pi}\right)^2\cdot\left(-\bar{\zeta}_2^{(0)}+\frac{1}{2}\cdot\bar{\zeta}_2^{(2)}\right), \tag{52}$$

where $\zeta_1^{(1)}$ has already been given in (36), so that m is a positive integer excepting 1.

By use of (47) and (49), (52) becomes

$$\zeta_1^{(m)}=\frac{(-1)^m}{(m\pi)^2}\cdot\frac{(kd)^3}{Q_1}\cdot(-2Q_3+Q_4)\qquad(m=2,\ 3,\ 4,\ \cdots)\ , \tag{53}$$

where Q_1, Q_3 and Q_4 have already been given in (33), (48) and (50) respectively.

Then the waves in the domain D_1 (in the part of the canal) are expressed (refer to paper I) as

$$\zeta_1=\sum_{m=0}^{\infty}\zeta_1^{(m)}\cos\frac{m\pi}{d}x\cdot\exp\left(-ik_1^{(m)}y\right), \tag{54}$$

where

$$k_1^{(m)}=\sqrt{k^2-\left(\frac{m\pi}{d}\right)^2}. \tag{55}$$

Next, the numerical calculations and the discussions of the results are made in the following.

Firstly, the behaviors of the waves in the part of the canal are examined numerically by use of (32), (36), (53) and (54).

When $kd<\pi$, the modes of the waves excepting the zeroth one are the waves damping out as the advancing waves depart from the mouth of the canal, because the expression (55) becomes imaginary for $kd<\pi$. In the present approximation, the application range might be considered to be limited to the range $kd<\pi$, so that the only zeroth mode of ζ_1 is propagated into the canal without damping. The variations of $|\zeta_1^{(0)}|$ (the absolute value of the non-damping wave in the canal) and $|\zeta_1^{(m)}|$ (the absolute values of the factors of the damping modes) are shown in Fig. 2,

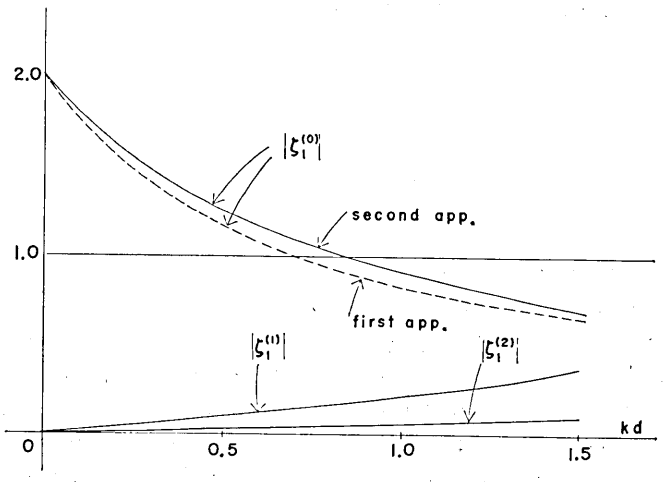

Fig. 2. Variations of the amplitudes of each mode in the canal versus kd (unit: ζ_0; the broken line stands for the curve obtained in paper I).

of which the values are tabulated in Table 1. In Fig. 2, the inserted broken line stands for the zeroth mode calculated in the previous paper I, of which the theory is derived under the linear approximation of the Bessel functions.

When the approximation proceeds from the first to the second one, the curve $|\zeta_1^{(0)}/\zeta_0|$ is uplifted a little, so that the interpretation is more acceptable that the occurrence of the intersection of the curve with a line $|\zeta_1^{(0)}/\zeta_0|=1.0$ in the former theory[4] is caused by a deficiency of the approximation, but the intersection of the curves still takes place which might be explained by the procedure analogous to that in paper I, i.e. an estimation of the errors due to the approximation (which is not made in the present purview).

Before proceeding with the discussions of the behaviors of the waves in the canal, the complete form of the waves in this part is described hereunder.

Allowing for the omitted time factor $\exp(-i\omega t)$ and taking the real part, the complete form for the waves in the domain D_1 becomes, from (54),

$$\zeta_1=\zeta_1^{(\mathrm{adv})}+\zeta_1^{(\mathrm{dam})}\ , \tag{56}$$

$$\left.\begin{aligned}\zeta_1^{(\mathrm{adv})} &=|\zeta_1^{(0)}|\cos(\omega t+ky-\arg.\zeta_1^{(0)})\\ \text{or}\quad &=|\zeta_1^{(0)}|\cos\{\omega t+k^*(y^*-\beta)\}\end{aligned}\right\}, \tag{57}$$

$$\zeta_1^{(\mathrm{dam})}=\sum_{m=0}^{\infty}|\zeta_1^{(m)}|\cos(\omega t-\arg.\zeta_1^{(m)})\cos\frac{m\pi}{d}x\cdot\exp(|k_1^{(m)}|y) \tag{58}$$

$$(y<0)\ ,$$

where

$$\left.\begin{aligned}k^*&=kd\ ,\qquad y^*=y/d\ ,\\ \beta&=(\arg.\zeta_1^{(0)})/kd\ .\end{aligned}\right\} \tag{59}$$

In the above expressions, $\zeta_1^{(\mathrm{adv})}$ and $\zeta_1^{(\mathrm{dam})}$ stand for the advancing and the damping waves respectively.

As already mentioned in paper I, the former of (57) is convenient to examine the phase difference at the mouth ($y=0$) of the canal, while the latter to inspect a supposed origin of the $\cos(\omega t+ky)$-type wave.

Since the variation of the amplitude $|\zeta_1^{(0)}|$ of the advancing waves $\zeta_1^{(\mathrm{adv})}$ for the second approximation nearly resembles that for the theory of the first order (see Fig. 2), the explanation for the advancing waves

4) T. MOMOI, *loc. cit.*, *1*).

is terminated to the extent that the upheaving of the curve is rather unexpectedly small in amount, hence details of the discussion is submitted to paper I.

When the approximation proceeds, the higher modes appear in magnitude which cannot be neglected, the variations of which are shown in Fig. 2 only for the first two modes, i.e., $|\zeta_1^{(1)}/\zeta_0|$ and $|\zeta_1^{(2)}/\zeta_0|$, other modes not being depicted because of the smallness of the values. When kd is small, the contributions of the higher modes to the waves in the canal are also small. As kd increases, these values are augmented almost linearly until the first mode at $kd=1.0$ amounts to about 21 percent of the zeroth one and the second mode about 5 percent. Such augmentations of the higher modes for growth of kd is physically accepted.

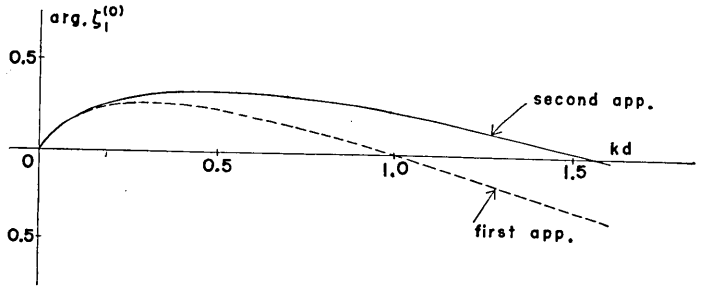

Fig. 3. A variation of the phase of the advancing mode in the canal versus kd (the broken line denotes the curve obtained in paper I).

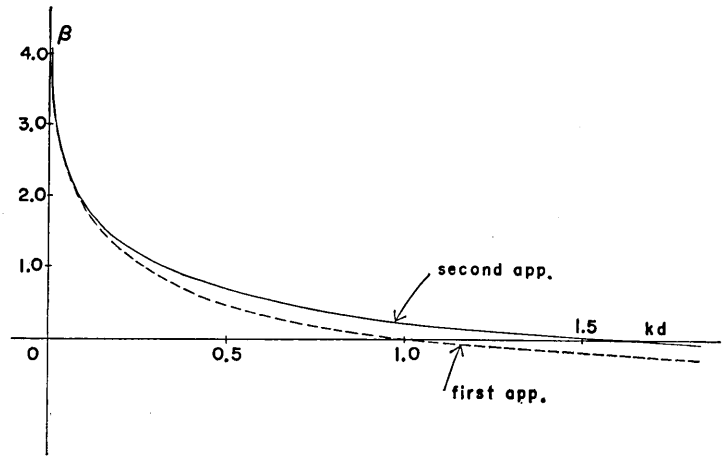

Fig. 4. A variation of a supposed origin of the $\cos(\omega t+ky)$-type wave in the canal versus kd (the broken line stands for curve obtained in paper I).

Now let us consider the behaviors of the phases. The variations of the phases are drawn for arg. $\zeta_1^{(0)}$ in Fig. 3 and for β in Fig. 4, and these values are arranged in Table 1. In both figures, the inserted broken lines stand for the curves based on the theory of the first approximation in paper I. Though the curves under the first approximation cross the zero lines at $kd=1.0$, such intersections, judging from the computed results under the second approximation, seem to have occurred occasionally. As the approximation continues, the curves denoting the variations of arg. $\zeta_1^{(0)}$ and β are uplifted, but the characteristic features of these variations are little changed as compared with those in the first approximation. That is to say :— Arg. $\zeta_1^{(0)}$ takes a maximum value at a certain point apart from $kd=0$. On the lower side of this point, this quantity diminishes to zero, while, on the upper side, the value decreases monotonically until it takes a negative value. For the appearance of such a maximum, the physical interpretation in paper I is also useful such that, when a length (λ) of the incident waves is large compared with a width (d) of the canal, the advancing waves in the canal are motivated in phase with the incident waves and that, when λ decreases for d, the partial flow (diffraction) of the water mass into the canal occurs around two corners of the mouth of the canal to cause a phase lag of the advancing waves until such partial flow, when λ becomes further decreased

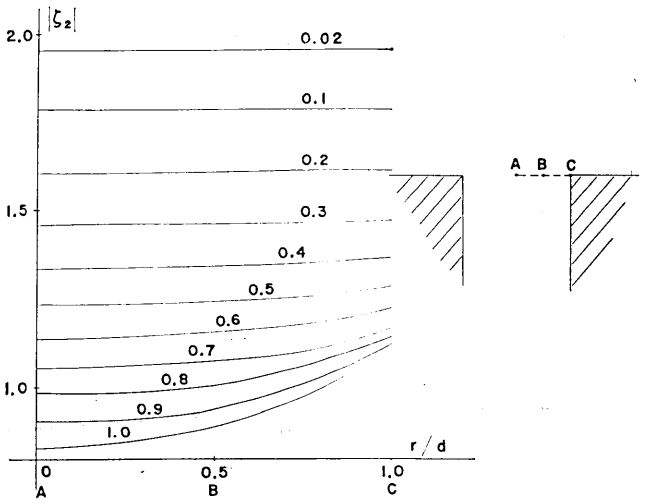

Fig. 5. A variation of the wave height in the direction $\theta=0$ versus r/d for a parameter kd in the range 0.02~1.0 (unit: ζ_0; characters A, B, C stated in the abscissa refer to the positions in the figure on the right-hand side).

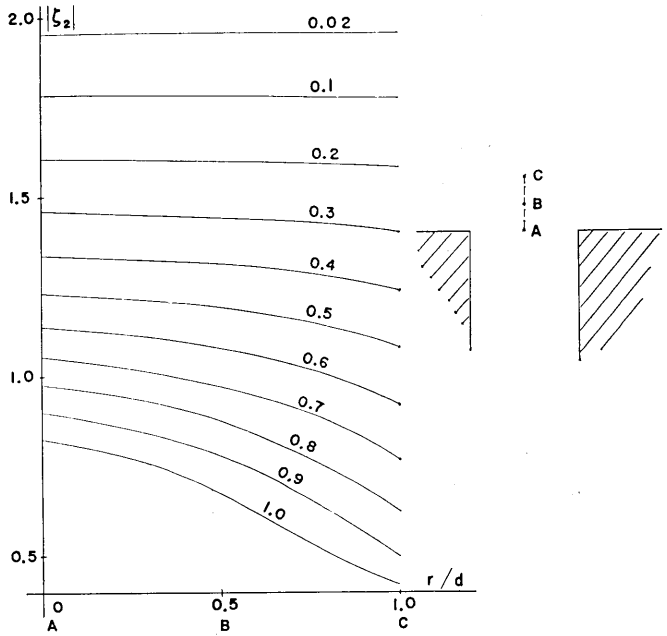

Fig. 6. A variation of the wave height in the direction of $\theta=\pi/2$ versus r/d for a parameter kd in the range 0.02~1.0 (unit: ζ_0; characters A, B, C stated in the abscissa refer to the positions in the figure on the right-hand side).

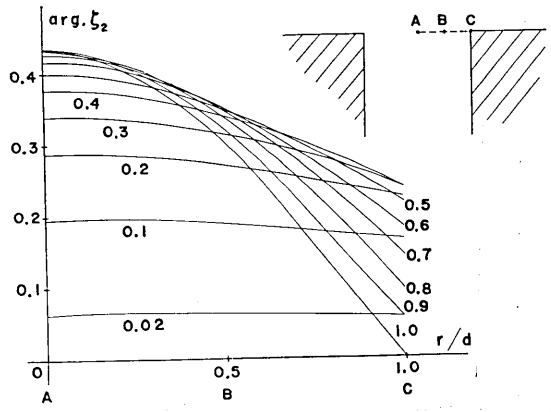

Fig. 7. A variation of the phase in the direction of $\theta=0$ versus r/d for a parameter kd in the range 0.02~1.0 (characters A, B, C stated in the abscissa refer to the positions in the figure on the upper side).

for d, hardly contributes to the invading waves. The last interpretation corresponds to the decrease of arg. $\zeta_1^{(0)}$ for large kd in Fig. 3.

As far as the variation of β is concerned, since this value denotes a hypothetical origin at which the $\cos(\omega t+ky)$-type waves in the canal originated, a supposed origin of these waves tends to an infinity for $kd\to 0$ and approaches to an estuary as kd increases (refer to Fig. 4).

Later, the overall pictures visualizing the variations of the wave height and the phase in site are given through two domains D_1 and D_2.

Now let us consider the waves in the domain D_2 in the following:

By use of the expressions (46), (47), (49) and (51), the wave heights and phases in the domain D_2 are calculated with the aid of an electronic

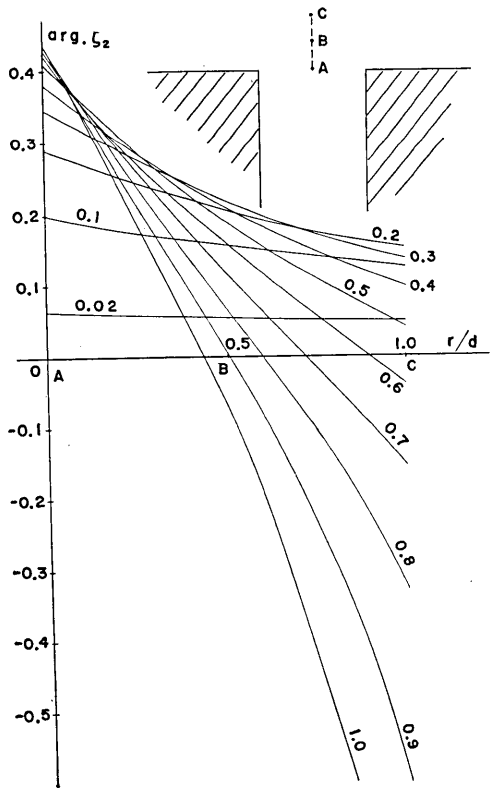

Fig. 8. A variation of the phase in the direction $\theta=\pi/2$ versus r/d for a parameter kd in the range 0.02~1.0 (characters A, B, C stated in the abscissa refer to the positions with the same letters in the figure on the upper side).

computer, the results of which are tabulated in Tables 2 and 3.

In this domain, our main interests are centered in the variations of the wave heights and phases in the directions $\theta=0$ and $\pi/2$. These figures are shown in Figs. 5, 6, 7, and 8 by using the values in Tables 2 and 3.

According to Figs. 5 and 6, when kd increases, the changes of the amplitudes for r/d are rapid as expected and the variations in the direction $\theta=\pi/2$ (Fig. 6) are larger than those in the direction $\theta=0$ (Fig. 5). This is considered to be due to the incidence of the invading waves perpendicular to the coast. When the site moves from the outer edge (C) of the domain to the central part (A), the wave height becomes greater for the former and smaller for the latter. For the range $kd>0.8$, the amplitudes at the central part (A) diminish below unity and this result seems to contradict our past experience. The appropriate explanation for this paradox might attribute to the deficiency of the present approximation.

For the variations of arg. ζ_2, the situation similar to that for $|\zeta_2/\zeta_0|$ is seen such that the changes of the phases towards $\theta=\pi/2$ are larger than in the direction $\theta=0$ (see Figs. 7 and 8). The phase shifts of the latter are considered to be caused by the diffraction of the waves around the estuary while, for the variations of the former, the primary cause is the direction of the incidence of the incoming waves to the coast, the secondary cause being a diffraction around the estuary.

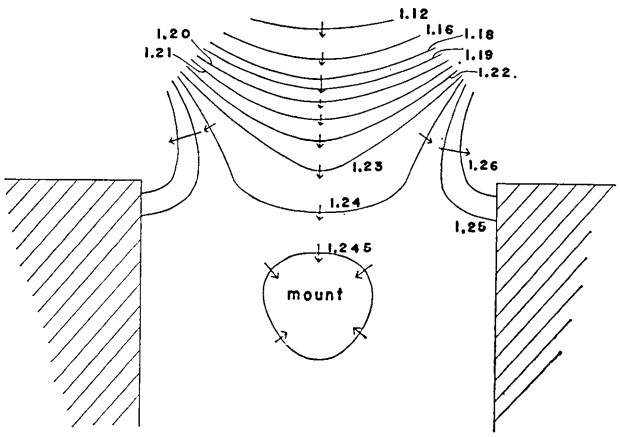

Fig. 9. Contours of the equi-amplitudes in the mouth of the canal for $kd=0.5$ (arrows drawn in the figure designate the directions of the positive gradient of the contours and the stated values stand for the magnitudes of the amplitudes).

Through Figs. 7 and 8, the phase lags in the central part (A) are greater than in the outer part (C). This fact suggests that the waves in this domain advance towards the central part (A). Furthermore, the advancing speeds are faster for the direction $\theta=\pi/2$ (Fig. 8) than those for $\theta=0$ (Fig. 7), judging from the gradients of the two figures.

Focussing our attention upon the behaviors of the phases in the nearby part of the center (A) in Fig. 7, the gradients of the curves in this region are very gentle as compared with those in the outer part (C). In other words, the waves in the direction $\theta=0$ get to stagnate when advancing towards the central part.

Now, let us give overall pictures showing the variations of the amplitudes and phases throughout two domains D_1 and D_2. In such explanations, the expressions used are (51) and (54). The number of terms taken up, in calculating the series (54), is up to $m=6$. Then the neglected first terms have been found, from numerical computations, to remain at a maximum of 10^{-3} for the range $kd=0$ to 1.0. The calculated amplitudes and phases in the domain D_1 are arranged in Tables 4 and 5, by use of which the behaviors of the waves in the part of the canal

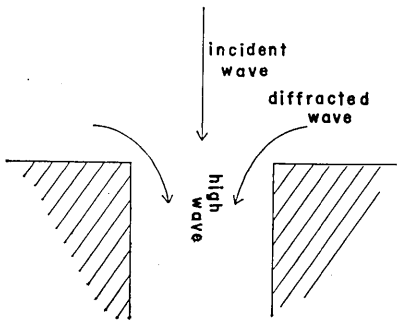

Fig. 10. A figurative explanation for the production of a small mount in the interior of the canal.

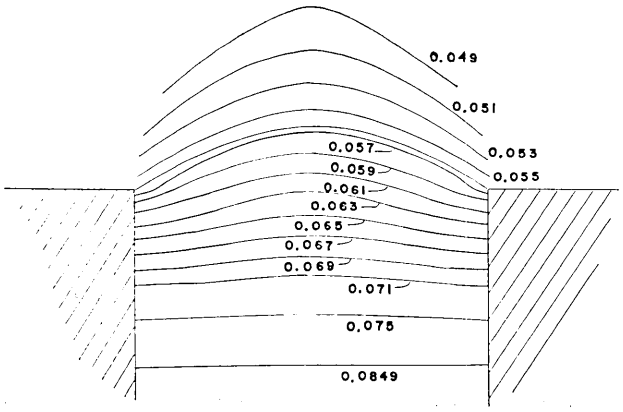

Fig. 11. Contours of the equi-phases in the mouth of the canal for $kd=0.02$ (the stated values denote the magnitudes of the phase lags).

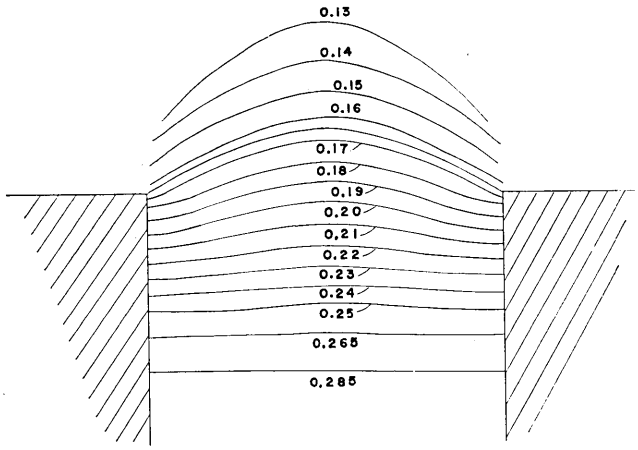

Fig. 12. Contours of the equi-phases in the mouth of the canal for kd=0.1 (the stated values stand for the magnitudes of the phase lags).

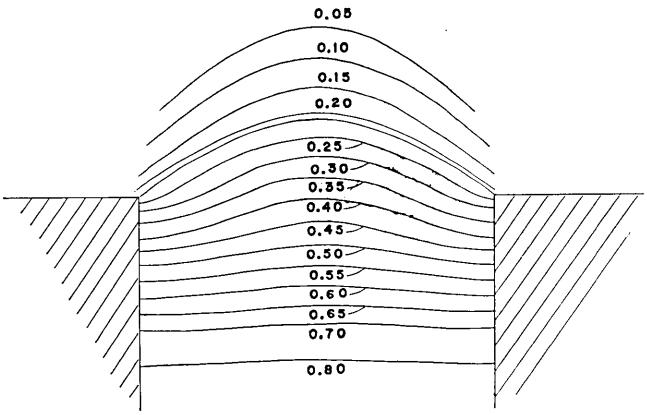

Fig. 13. Contours of the equi-phases in the mouth of the canal for kd=0.5 (the stated values stand for the magnitudes of the phase lags).

are visualized in Figs. 9, 11, 12 and 13 for specified values of kd, i.e., 0.5, 0.02, 0.1 and 0.5 in Figs. 9, 11, 12, and 13 respectively. Alternatively, the variations in the domain D_2 of these figures are depicted by using Tables 2 and 3 which have already been given before. If necessary, the figure for other specified values of kd can readily be drawn on the basis of the data in Tables 2 to 5.

To begin with, the explanation for Fig. 9 is given.

The most conspicuous feature in this figure is a generation of a

mount in the interior of the canal. Since our theory is developed under the assumption of uniform depth, such a mount is interpreted to be produced completely as a result of the diffraction of the waves around the estuary. As shown schematically in Fig. 10, the directly incident waves are superimposed by the diffracted waves from either corner of the mouth to cause high waves inside the canal.

Other features for the behaviors of the wave heights are such that :—

(1) The uniform decay of the wave height, near the corner, towards the canal seems to suggest a strong divergence of the diffracted waves (the waves are diffracted uniformly in space).

(2) The contours composed of equi-amplitudes, roughly speaking, make a hyperbola outside the canal. This tendency is anticipated from our past experience.

Although Fig. 9 represents the variation of the wave height for a specified value, i.e. $kd=0.5$, such characteristic features are considered to be still prevailing for other kd less than 1.0.

Now let us proceed with the explanations of Figs. 11, 12 and 13.

Throughout all the figures, the contours of the equi-phases are wedge-shaped (of a triangular form) at the outer margin of the domain D_2 (buffer domain). When approaching the canal, these contours begin to run parallel to the coastline until the equi-phase lines, in the interior of the channel, become completely straight and perpendicular to the axis of the canal. Furthermore, noting the transitions of the stated values, it is found that the waves in these domains are propagated into the canal such that they first advance towards the center ($(x, y)=(0, 0)$: the origin of the coordinate) of the mouth of the canal and, while progressing, gradually deform the direction of their propagation into a line with the axis of the canal.

In paper I, we have already stated that, provided that the linear approximations of sine and cosine functions are held for the quantities in the domain D_2, the wave in this region are propagated with their crests parallel to the coast facing the open sea. But, from the results of the present paper, such approximations are found to be too extreme for the analysis in the domain in front of the canal.

Through Figs. 11, 12 and 13, one more fact is seen such that the equi-phase lines are denser near the corner of the mouth of the canal than in the middle part. In other words, the waves in the former part advance more slowly than in the latter.

Finally, let us consider the behaviors of the waves in the open sea

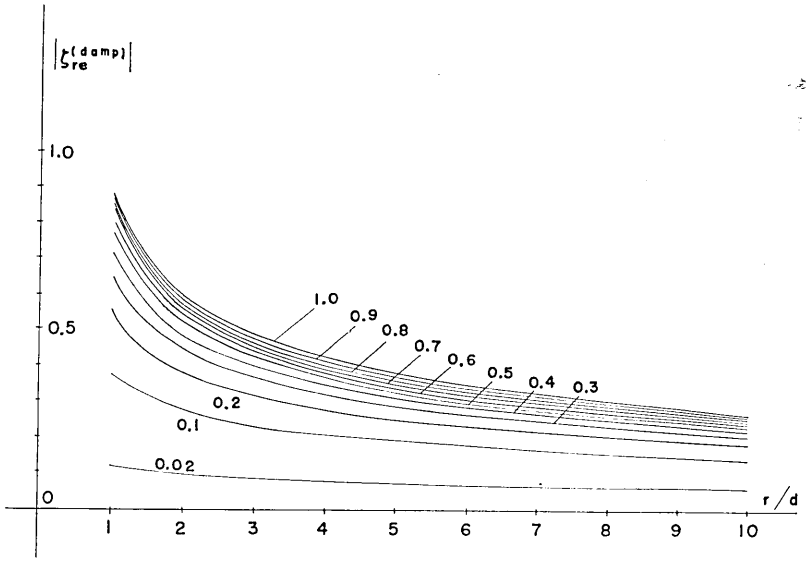

Fig. 14. Variations of the damping reflected waves in the direction of $\theta=0$ in the open sea versus a position r/d for parameters kd in the range 0.02 to 1.2 (the stated number in the figure stands for the curve relevant to the parameter kd of the referred value; unit: ζ_0).

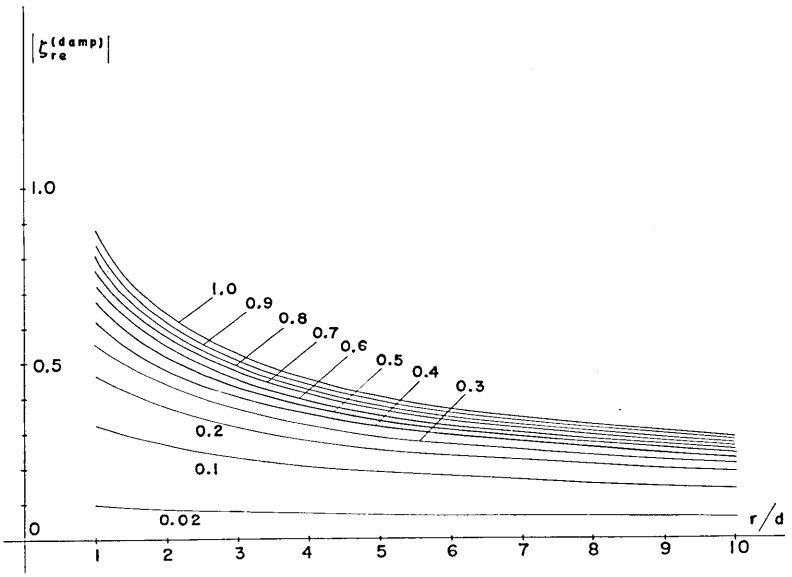

Fig. 15. Variations of the damping reflected waves in the direction of $\theta=\pi/4$ in the open sea versus a position r/d for parameters kd in the range 0.02 to 1.0 (the stated number in the figure stands for the curve relevant to the parameter kd of the referred value; unit: ζ_0).

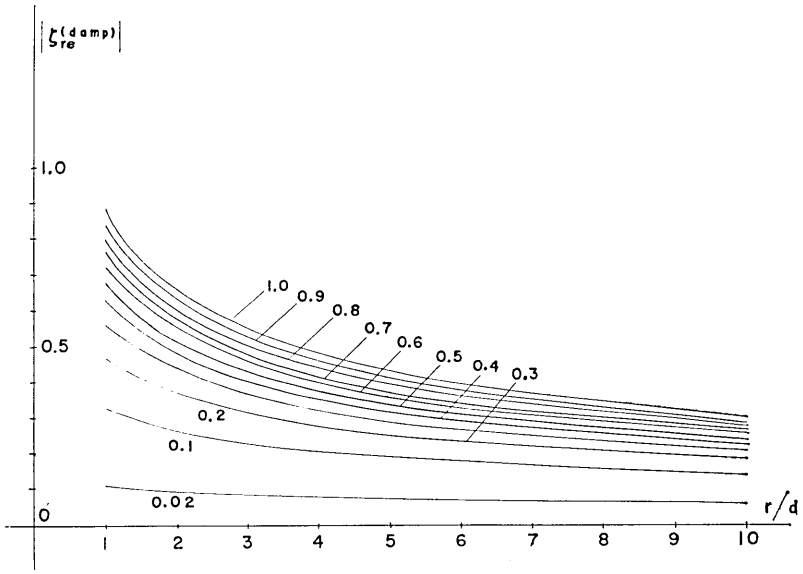

Fig. 16. Variations of the damping reflected waves in the direction of $\theta=\pi/2$ in the open sea versus a position r/d for parameters kd in the range 0.02 to 1.0 (the stated number in the figure stands for the curve relevant to the parameter kd of the referred value; unit: ζ_0).

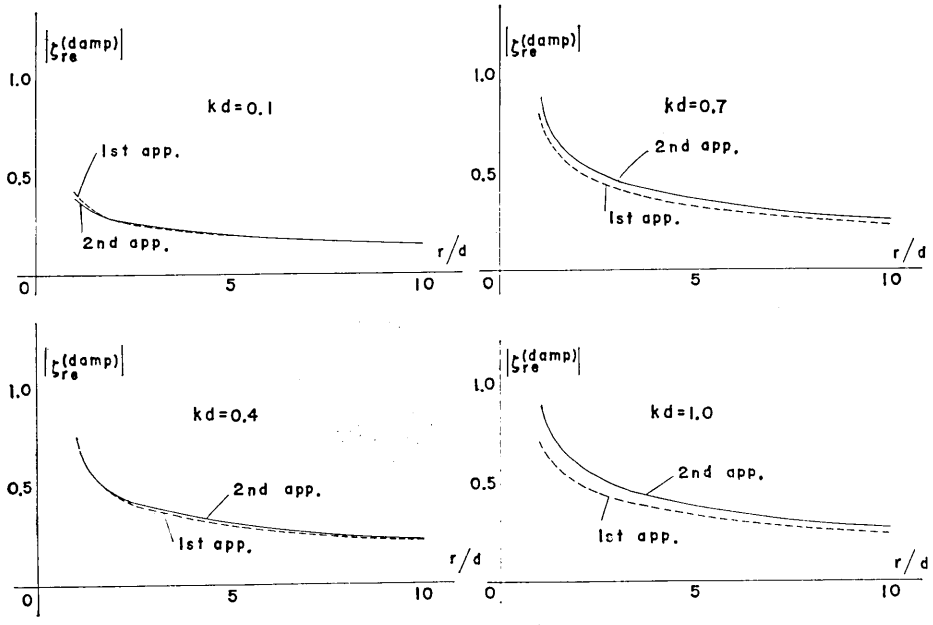

Fig. 17. Comparisons of the damping reflected waves in the direction $\theta=0$ in the open sea derived under the first and second approximations (unit: ζ_0).

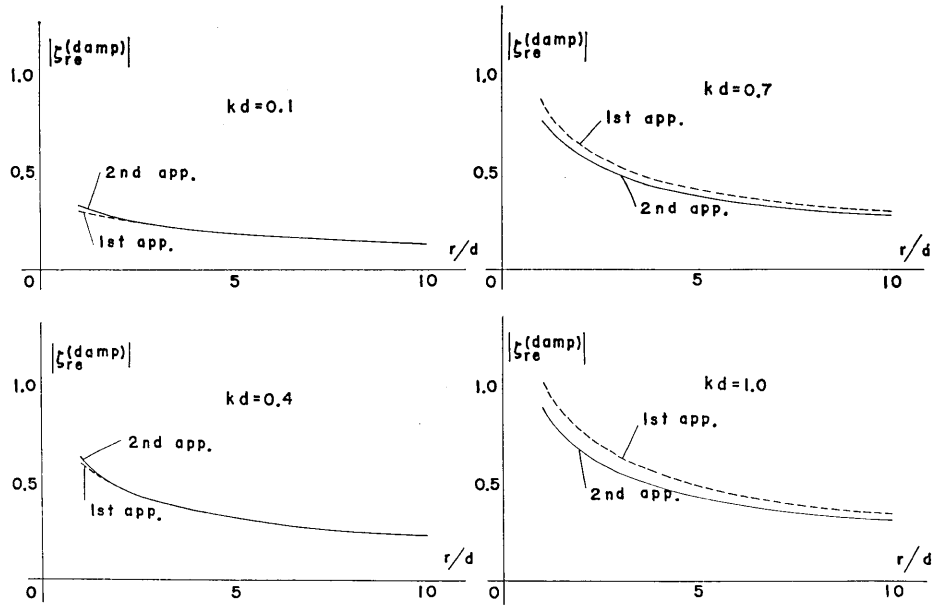

Fig. 18. Comparisons of the damping reflected waves in the direction $\theta=\pi/2$ in the open sea derived under the first and second approximations (unit: ζ_0).

(domain D_3).

In the domain D_3, our chief interest is the damping reflected waves $\zeta_{re}^{(damp)}$, which are examined numerically through the expression (45). The figures showing the variations of $\zeta_{re}^{(damp)}$ for position r/d (the direction θ taken parameter) are visualized in Figs. 14, 15 and 16 (the actual calculations of (45) have been made by use of an electronic computer).

Before proceeding with the detailed discussions, the convergence of two results obtained in paper I and this paper must be checked. These examinations are made in Figs. 17 and 18 for particular values $kd=0.1$, 0.4, 0.7 and 1.0, choosing two directions $\theta=0$ and $\pi/2$ as other parameters. In Figs. 17 and 18, the solid and broken lines stand for those relevant to the second and first approximations respectively (the former is for the present work and the latter for paper I). According to these figures, the agreements of two curves (for the first and second approximations) are fairly well up to about $kd=0.5$ except for a little departure near $r/d \approx 1.0$. As kd increases beyond about 0.5, the departures of the two curves become far from negligible in amount. But the main features of the damping reflected waves in the open sea do not become lost, though the approximation steps up from the first to the second one.

Viewing Figs. 14, 15, and 16, we find the following facts, some of which have already been observed in the previous study of paper I :—

For small kd, only a slight modification of the standing waves (the first term of (44)) by the damping reflected ones (the second term of (44)) is seen such that, when $kd=0.02$, the order of the modification is about 10 percent of the incident waves in the nearby part of an estuary ($r\approx d$) and less than 10 percent when departing from the mouth of the canal. When kd increases, the standing waves are more influenced by $\zeta_{re}^{(\mathrm{damp})}$. Along the coast ($\theta=0$), the contribution of $\zeta_{re}^{(\mathrm{damp})}$ at $kd=1.0$ amounts to 90 percent of the height of the incident waves near the estuary and 27 percent at $r/d=10.0$. As θ increases (a line tracing the variation of the wave height is directed in a sense perpendicular to the coastline), the heights of the damping reflected waves are slightly upheaved. But such upheavals are small in amount as compared with those obtained in paper I, of which the theory was developed under the linear approximations of the Bessel functions. The generalization of the approximation from the first to the second one results in smoothing the directivity of the damping reflected waves.

As far as the damping rate of $\zeta_{re}^{(\mathrm{damp})}$ is concerned, when kd is small (a wavelength of the incident waves is long as compared with a width of the canal), the rate of the damping is very gentle, as is to be expected, while, as kd increases, this rate also increases particularly in the nearby region of the estuary, the damping rate being larger along the coast than towards the offing.

Furthermore, one more outstanding feature, though we have already mentioned it in paper I, is found such that the surface composed of the amplitudes of the damping reflected waves tends to an asymptotic one as kd increases.

Since the variations of the damping reflected waves in the second approximation resemble those obtained under the first approximation, the computed values are not presented in the present purview.

Table 1. The variations of the waves in the domain D_1 versus kd.*)

kd	$\lvert\zeta_1^{(0)}/\zeta_0\rvert$	arg. $\zeta_1^{(0)}$	β	$\lvert\zeta_1^{(1)}/\zeta_0\rvert$	arg. $\zeta_1^{(1)}$
0.02	1.9572	0.06061	3.03053	0.00505	−1.5098
0.1	1.7865	0.18616	1.86166	0.02342	−1.3768
0.2	1.6065	0.26554	1.32771	0.04360	−1.2751
0.3	1.4616	0.30671	1.02238	0.06223	−1.1985
0.4	1.3431	0.32631	0.81578	0.08031	−1.1321
0.5	1.2438	0.33175	0.66349	0.09843	−1.0698
0.6	1.1587	0.32684	0.54473	0.11701	−1.0088
0.7	1.0844	0.31377	0.44824	0.13637	−0.9475
0.8	1.0184	0.29387	0.36734	0.15685	−0.8852
0.9	0.9588	0.26807	0.29786	0.17876	−0.8212
1.0	0.9045	0·23709	0.23709	0.20244	−0.7549
1.1	0.8542	0.20158	0.18325	0.22826	−0.6852
1.2	0.8073	0.16221	0.13518	0.25667	−0.6106
1.3	0.7632	0.11971	0.09209	0.28818	−0.5286
1.4	0.7215	0.07485	0.05347	0.32360	−0.4344
1.5	0.6821	0.02846	0.01897	0.36448	−0.3196

*) The calculation of the higher mode has been made only for the first mode of the waves and the other higher modes are readily calculated by use of (52) and the above values.

Table 2. The variation of the ampliudes in the domain D_2.

When $kd=0.02$,

r/d \ θ (rad.)	0	$\pi/10$	$\pi/5$	$3\pi/10$	$2\pi/5$	$\pi/2$
0.0	0.1957×10^{1}	0.1957×10^{1}	0.1957×10^{1}	0.1957×10^{1}	0.1957×10^{1}	0.1957×10^{1}
0.2	0.1957×10^{1}	0.1957×10^{1}	0.1957×10^{1}	0.1957×10^{1}	0.1957×10^{1}	0.1957×10^{1}
0.4	0.1957×10^{1}	0.1957×10^{1}	0.1957×10^{1}	0.1957×10^{1}	0.1957×10^{1}	0.1957×10^{1}
0.6	0.1957×10^{1}	0.1957×10^{1}	0.1957×10^{1}	0.1957×10^{1}	0.1957×10^{1}	0.1957×10^{1}
0.8	0.1957×10^{1}	0.1957×10^{1}	0.1957×10^{1}	0.1957×10^{1}	0.1957×10^{1}	0.1957×10^{1}
1.0	0.1957×10^{1}	0.1957×10^{1}	0.1957×10^{1}	0.1957×10^{1}	0.1957×10^{1}	0.1957×10^{1}

When $kd=0.1$,

r/d \ θ (rad.)	0	$\pi/10$	$\pi/5$	$3\pi/10$	$2\pi/5$	$\pi/2$
0.0	0.1786×10^{1}	0.1786×10^{1}	0.1786×10^{1}	0.1786×10^{1}	0.1786×10^{1}	0.1786×10^{1}
0.2	0.1786×10^{1}	0.1786×10^{1}	0.1786×10^{1}	0.1786×10^{1}	0.1786×10^{1}	0.1786×10^{1}
0.4	0.1786×10^{1}	0.1786×10^{1}	0.1786×10^{1}	0.1786×10^{1}	0.1785×10^{1}	0.1785×10^{1}
0.6	0.1787×10^{1}	0.1786×10^{1}	0.1786×10^{1}	0.1785×10^{1}	0.1785×10^{1}	0.1784×10^{1}
0.8	0.1787×10^{1}	0.1787×10^{1}	0.1786×10^{1}	0.1785×10^{1}	0.1783×10^{1}	0.1782×10^{1}
1.0	0.1787×10^{1}	0.1788×10^{1}	0.1786×10^{1}	0.1784×10^{1}	0.1781×10^{1}	0.1780×10^{1}

When $kd=0.2$,

r/d \ θ (rad.)	0	$\pi/10$	$\pi/5$	$3\pi/10$	$2\pi/5$	$\pi/2$
0.0	0.1606×10^{1}	0.1606×10^{1}	0.1606×10^{1}	0.1606×10^{1}	0.1606×10^{1}	0.1606×10^{1}
0.2	0.1606×10^{1}	0.1605×10^{1}	0.1605×10^{1}	0.1605×10^{1}	0.1604×10^{1}	0.1604×10^{1}
0.4	0.1606×10^{1}	0.1605×10^{1}	0.1604×10^{1}	0.1603×10^{1}	0.1602×10^{1}	0.1602×10^{1}
0.6	0.1606×10^{1}	0.1606×10^{1}	0.1604×10^{1}	0.1601×10^{1}	0.1598×10^{1}	0.1597×10^{1}
0.8	0.1607×10^{1}	0.1608×10^{1}	0.1605×10^{1}	0.1598×10^{1}	0.1592×10^{1}	0.1590×10^{1}
1.0	0.1610×10^{1}	0.1612×10^{1}	0.1606×10^{1}	0.1595×10^{1}	0.1584×10^{1}	0.1580×10^{1}

When $kd=0.3$,

r/d \ θ (rad.)	0	$\pi/10$	$\pi/5$	$3\pi/10$	$2\pi/5$	$\pi/2$
0.0	0.1459×10^{1}	0.1459×10^{1}	0.1459×10^{1}	0.1459×10^{1}	0.1459×10^{1}	0.1459×10^{1}
0.2	0.1459×10^{1}	0.1459×10^{1}	0.1458×10^{1}	0.1457×10^{1}	0.1456×10^{1}	0.1456×10^{1}
0.4	0.1460×10^{1}	0.1459×10^{1}	0.1456×10^{1}	0.1453×10^{1}	0.1451×10^{1}	0.1449×10^{1}
0.6	0.1462×10^{1}	0.1461×10^{1}	0.1456×10^{1}	0.1449×10^{1}	0.1442×10^{1}	0.1439×10^{1}
0.8	0.1465×10^{1}	0.1466×10^{1}	0.1458×10^{1}	0.1443×10^{1}	0.1429×10^{1}	0.1424×10^{1}
1.0	0.1472×10^{1}	0.1475×10^{1}	0.1461×10^{1}	0.1435×10^{1}	0.1412×10^{1}	0.1403×10^{1}

(to be continued)

When $kd=0.4$, (continued)

r/d \ θ (rad.)	0	$\pi/10$	$\pi/5$	$3\pi/10$	$2\pi/5$	$\pi/2$
0.0	0.1337×10^{1}	0.1337×10^{1}	0.1337×10^{1}	0.1337×10^{1}	0.1337×10^{1}	0.1337×10^{1}
0.2	0.1338×10^{1}	0.1336×10^{1}	0.1335×10^{1}	0.1333×10^{1}	0.1331×10^{1}	0.1331×10^{1}
0.4	0.1340×10^{1}	0.1337×10^{1}	0.1333×10^{1}	0.1327×10^{1}	0.1322×10^{1}	0.1321×10^{1}
0.6	0.1344×10^{1}	0.1341×10^{1}	0.1333×10^{1}	0.1319×10^{1}	0.1307×10^{1}	0.1303×10^{1}
0.8	0.1351×10^{1}	0.1351×10^{1}	0.1336×10^{1}	0.1309×10^{1}	0.1285×10^{1}	0.1276×10^{1}
1.0	0.1364×10^{1}	0.1368×10^{1}	0.1342×10^{1}	0.1296×10^{1}	0.1255×10^{1}	0.1238×10^{1}

When $kd=0.5$,

r/d \ θ (rad.)	0	$\pi/10$	$\pi/5$	$3\pi/10$	$2\pi/5$	$\pi/2$
0.0	0.1233×10^{1}	0.1233×10^{1}	0.1233×10^{1}	0.1233×10^{1}	0.1233×10^{1}	0.1233×10^{1}
0.2	0.1234×10^{1}	0.1231×10^{1}	0.1228×10^{1}	0.1226×10^{1}	0.1224×10^{1}	0.1222×10^{1}
0.4	0.1238×10^{1}	0.1233×10^{1}	0.1225×10^{1}	0.1216×10^{1}	0.1208×10^{1}	0.1206×10^{1}
0.6	0.1245×10^{1}	0.1241×10^{1}	0.1226×10^{1}	0.1205×10^{1}	0.1186×10^{1}	0.1178×10^{1}
0.8	0.1258×10^{1}	0.1257×10^{1}	0.1231×10^{1}	0.1189×10^{1}	0.1152×10^{1}	0.1137×10^{1}
1.0	0.1281×10^{1}	0.1285×10^{1}	0.1243×10^{1}	0.1171×10^{1}	0.1106×10^{1}	0.1081×10^{1}

When $kd=0.6$,

r/d \ θ (rad.)	0	$\pi/10$	$\pi/5$	$3\pi/10$	$2\pi/5$	$\pi/2$
0.0	0.1141×10^{1}	0.1141×10^{1}	0.1141×10^{1}	0.1141×10^{1}	0.1141×10^{1}	0.1141×10^{1}
0.2	0.1142×10^{1}	0.1138×10^{1}	0.1134×10^{1}	0.1130×10^{1}	0.1127×10^{1}	0.1125×10^{1}
0.4	0.1148×10^{1}	0.1142×10^{1}	0.1131×10^{1}	0.1117×10^{1}	0.1106×10^{1}	0.1101×10^{1}
0.6	0.1161×10^{1}	0.1154×10^{1}	0.1132×10^{1}	0.1100×10^{1}	0.1073×10^{1}	0.1062×10^{1}
0.8	0.1182×10^{1}	0.1178×10^{1}	0.1141×10^{1}	0.1080×10^{1}	0.1026×10^{1}	0.1004×10^{1}
1.0	0.1216×10^{1}	0.1220×10^{1}	0.1157×10^{1}	0.1055×10^{1}	0.9625×10^{0}	0.9258×10^{0}

When $kd=0.7$,

r/d \ θ (rad.)	0	$\pi/10$	$\pi/5$	$3\pi/10$	$2\pi/5$	$\pi/2$
0.0	0.1057×10^{1}	0.1057×10^{1}	0.1057×10^{1}	0.1057×10^{1}	0.1057×10^{1}	0.1057×10^{1}
0.2	0.1059×10^{1}	0.1054×10^{1}	0.1048×10^{1}	0.1042×10^{1}	0.1037×10^{1}	0.1036×10^{1}
0.4	0.1068×10^{1}	0.1059×10^{1}	0.1044×10^{1}	0.1024×10^{1}	0.1008×10^{1}	0.1002×10^{1}
0.6	0.1087×10^{1}	0.1077×10^{1}	0.1047×10^{1}	0.1003×10^{1}	0.9646×10^{0}	0.9495×10^{0}
0.8	0.1119×10^{1}	0.1113×10^{1}	0.1059×10^{1}	0.9766×10^{0}	0.9031×10^{0}	0.8738×10^{0}
1.0	0.1170×10^{1}	0.1171×10^{1}	0.1085×10^{1}	0.9463×10^{0}	0.8226×10^{0}	0.7736×10^{0}

(to be continued)

When $kd=0.8$, (continued)

r/d \ θ (rad.)	0	$\pi/10$	$\pi/5$	$3\pi/10$	$2\pi/5$	$\pi/2$
0.0	0.9786×10^{0}	0.9786×10^{0}	0.9786×10^{0}	0.9786×10^{0}	0.9786×10^{0}	0.9786×10^{0}
0.2	0.9826×10^{0}	0.9755×10^{0}	0.9673×10^{0}	0.9592×10^{0}	0.9532×10^{0}	0.9509×10^{0}
0.4	0.9959×10^{0}	0.9836×10^{0}	0.9623×10^{0}	0.9364×10^{0}	0.9150×10^{0}	0.9067×10^{0}
0.6	0.1022×10^{1}	0.1009×10^{1}	0.9672×10^{0}	0.9093×10^{0}	0.8591×10^{0}	0.8393×10^{0}
0.8	0.1067×10^{1}	0.1057×10^{1}	0.9858×10^{0}	0.8781×10^{0}	0.7833×10^{0}	0.7458×10^{0}
1.0	0.1138×10^{1}	0.1135×10^{1}	0.1021×10^{1}	0.8448×10^{0}	0.6893×10^{0}	0.6280×10^{0}

When $kd=0.9$,

r/d \ θ (rad.)	0	$\pi/10$	$\pi/5$	$3\pi/10$	$2\pi/5$	$\pi/2$
0.0	0.9036×10^{0}	0.9036×10^{0}	0.9036×10^{0}	0.9036×10^{0}	0.9036×10^{0}	0.9036×10^{0}
0.2	0.9092×10^{0}	0.9001×10^{0}	0.8895×10^{0}	0.8789×10^{0}	0.8711×10^{0}	0.8682×10^{0}
0.4	0.9277×10^{0}	0.9117×10^{0}	0.8840×10^{0}	0.8506×10^{0}	0.8232×10^{0}	0.8126×10^{0}
0.6	0.9644×10^{0}	0.9461×10^{0}	0.8922×10^{0}	0.8185×10^{0}	0.7553×10^{0}	0.7305×10^{0}
0.8	0.1026×10^{1}	0.1011×10^{1}	0.9186×10^{0}	0.7843×10^{0}	0.6680×10^{0}	0.6225×10^{0}
1.0	0.1121×10^{1}	0.1111×10^{1}	0.9671×10^{0}	0.7529×10^{0}	0.5710×10^{0}	0.5018×10^{0}

When $kd=1.0$,

r/d \ θ (rad.)	0	$\pi/10$	$\pi/5$	$3\pi/10$	$2\pi/5$	$\pi/2$
0.0	0.8299×10^{0}	0.8299×10^{0}	0.8299×10^{0}	0.8299×10^{0}	0.8299×10^{0}	0.8299×10^{0}
0.2	0.8375×10^{0}	0.8262×10^{0}	0.8128×10^{0}	0.7999×10^{0}	0.7898×10^{0}	0.7862×10^{0}
0.4	0.8627×10^{0}	0.8425×10^{0}	0.8077×10^{0}	0.7661×10^{0}	0.7321×10^{0}	0.7190×10^{0}
0.6	0.9119×10^{0}	0.8882×10^{0}	0.8207×10^{0}	0.7302×10^{0}	0.6537×10^{0}	0.6239×10^{0}
0.8	0.9936×10^{0}	0.9713×10^{0}	0.8573×10^{0}	0.6968×10^{0}	0.5623×10^{0}	0.5111×10^{0}
1.0	0.1115×10^{1}	0.1097×10^{1}	0.9211×10^{0}	0.6751×10^{0}	0.4864×10^{0}	0.4253×10^{0}

Table 3. The variation of the phases in the domain D_2.

When $kd=0.02$,

r/d \ θ (rad.)	0	$\pi/10$	$\pi/5$	$3\pi/10$	$2\pi/5$	$\pi/2$
0.0	0.6273×10^{-1}	0.6273×10^{-1}	0.6273×10^{-1}	0.6273×10^{-1}	0.6273×10^{-1}	0.6273×10^{-1}
0.2	0.6248×10^{-1}	0.6129×10^{-1}	0.6030×10^{-1}	0.5957×10^{-1}	0.5914×10^{-1}	0.5898×10^{-1}
0.4	0.6171×10^{-1}	0.5943×10^{-1}	0.5771×10^{-1}	0.5657×10^{-1}	0.5595×10^{-1}	0.5575×10^{-1}
0.6	0.6044×10^{-1}	0.5717×10^{-1}	0.5497×10^{-1}	0.5373×10^{-1}	0.5317×10^{-1}	0.5302×10^{-1}
0.8	0.5865×10^{-1}	0.5449×10^{-1}	0.5206×10^{-1}	0.5105×10^{-1}	0.5081×10^{-1}	0.5081×10^{-1}
1.0	0.5636×10^{-1}	0.5139×10^{-1}	0.4901×10^{-1}	0.4852×10^{-1}	0.4886×10^{-1}	0.4911×10^{-1}

When $kd=0.1$,

r/d \ θ (rad.)	0	$\pi/10$	$\pi/5$	$3\pi/10$	$2\pi/5$	$\pi/2$
0.0	0.1969×10^{0}	0.1969×10^{0}	0.1969×10^{0}	0.1969×10^{0}	0.1969×10^{0}	0.1969×10^{0}
0.2	0.1956×10^{0}	0.1897×10^{0}	0.1848×10^{0}	0.1811×10^{0}	0.1789×10^{0}	0.1782×10^{0}
0.4	0.1917×10^{0}	0.1804×10^{0}	0.1718×10^{0}	0.1662×10^{0}	0.1630×10^{0}	0.1621×10^{0}
0.6	0.1853×10^{0}	0.1690×10^{0}	0.1581×10^{0}	0.1519×10^{0}	0.1492×10^{0}	0.1485×10^{0}
0.8	0.1762×10^{0}	0.1554×10^{0}	0.1435×10^{0}	0.1385×10^{0}	0.1374×10^{0}	0.1375×10^{0}
1.0	0.1646×10^{0}	0.1399×10^{0}	0.1281×10^{0}	0.1258×10^{0}	0.1277×10^{0}	0.1290×10^{0}

When $kd=0.2$,

r/d \ θ (rad.)	0	$\pi/10$	$\pi/5$	$3\pi/10$	$2\pi/5$	$\pi/2$
0.0	0.2880×10^{0}	0.2880×10^{0}	0.2880×10^{0}	0.2880×10^{0}	0.2880×10^{0}	0.2880×10^{0}
0.2	0.2853×10^{0}	0.2735×10^{0}	0.2636×10^{0}	0.2564×10^{0}	0.2521×10^{0}	0.2506×10^{0}
0.4	0.2773×10^{0}	0.2546×10^{0}	0.2376×10^{0}	0.2264×10^{0}	0.2204×10^{0}	0.2185×10^{0}
0.6	0.2639×10^{0}	0.2314×10^{0}	0.2098×10^{0}	0.1980×10^{0}	0.1928×10^{0}	0.1914×10^{0}
0.8	0.2451×10^{0}	0.2039×10^{0}	0.1804×10^{0}	0.1710×10^{0}	0.1692×10^{0}	0.1694×10^{0}
1.0	0.2212×10^{0}	0.1722×10^{0}	0.1493×10^{0}	0.1454×10^{0}	0.1497×10^{0}	0.1524×10^{0}

When $kd=0.3$,

r/d \ θ (rad.)	0	$\pi/10$	$\pi/5$	$3\pi/10$	$2\pi/5$	$\pi/2$
0.0	0.3424×10^{0}	0.3424×10^{0}	0.3424×10^{0}	0.3424×10^{0}	0.3424×10^{0}	0.3424×10^{0}
0.2	0.3381×10^{0}	0.3204×10^{0}	0.3057×10^{0}	0.2949×10^{0}	0.2885×10^{0}	0.2863×10^{0}
0.4	0.3255×10^{0}	0.2916×10^{0}	0.2663×10^{0}	0.2498×10^{0}	0.2409×10^{0}	0.2382×10^{0}
0.6	0.3046×10^{0}	0.2560×10^{0}	0.2242×10^{0}	0.2069×10^{0}	0.1995×10^{0}	0.1976×10^{0}
0.8	0.2753×10^{0}	0.2138×10^{0}	0.1794×10^{0}	0.1659×10^{0}	0.1637×10^{0}	0.1642×10^{0}
1.0	0.2378×10^{0}	0.1654×10^{0}	0.1320×10^{0}	0.1267×10^{0}	0.1336×10^{0}	0.1379×10^{0}

(to be continued)

When $kd=0.4$, (continued)

r/d \ θ (rad.)	0	$\pi/10$	$\pi/5$	$3\pi/10$	$2\pi/5$	$\pi/2$
0.0	0.3771×10^{0}	0.3771×10^{0}	0.3771×10^{0}	0.3771×10^{0}	0.3771×10^{0}	0.3771×10^{0}
0.2	0.3712×10^{0}	0.3474×10^{0}	0.3279×10^{0}	0.3137×10^{0}	0.3052×10^{0}	0.3023×10^{0}
0.4	0.3534×10^{0}	0.3083×10^{0}	0.2749×10^{0}	0.2533×10^{0}	0.2416×10^{0}	0.2381×10^{0}
0.6	0.3241×10^{0}	0.2597×10^{0}	0.2179×10^{0}	0.1954×10^{0}	0.1857×10^{0}	0.1834×10^{0}
0.8	0.2833×10^{0}	0.2022×10^{0}	0.1571×10^{0}	0.1395×10^{0}	0.1368×10^{0}	0.1376×10^{0}
1.0	0.2316×10^{0}	0.1366×10^{0}	0.9274×10^{-1}	0.8528×10^{-1}	0.9418×10^{-1}	0.9998×10^{-1}

When $kd=0.5$,

r/d \ θ (rad.)	0	$\pi/10$	$\pi/5$	$3\pi/10$	$2\pi/5$	$\pi/2$
0.0	0.4001×10^{0}	0.4001×10^{0}	0.4001×10^{0}	0.4001×10^{0}	0.4001×10^{0}	0.4001×10^{0}
0.2	0.3923×10^{0}	0.3626×10^{0}	0.3383×10^{0}	0.3205×10^{0}	0.3099×10^{0}	0.3064×10^{0}
0.4	0.3688×10^{0}	0.3125×10^{0}	0.2710×10^{0}	0.2443×10^{0}	0.2299×10^{0}	0.2255×10^{0}
0.6	0.3301×10^{0}	0.2501×10^{0}	0.1984×10^{0}	0.1705×10^{0}	0.1585×10^{0}	0.1555×10^{0}
0.8	0.2768×10^{0}	0.1766×10^{0}	0.1207×10^{0}	0.9825×10^{-1}	0.9427×10^{-1}	0.9495×10^{-1}
1.0	0.2103×10^{0}	0.9393×10^{-1}	0.3872×10^{-1}	0.2659×10^{-1}	0.3538×10^{-1}	0.4195×10^{-1}

When $kd=0.6$,

r/d \ θ (rad.)	0	$\pi/10$	$\pi/5$	$3\pi/10$	$2\pi/5$	$\pi/2$
0.0	0.4156×10^{0}	0.4156×10^{0}	0.4156×10^{0}	0.4156×10^{0}	0.4156×10^{0}	0.4156×10^{0}
0.2	0.4056×10^{0}	0.3699×10^{0}	0.3407×10^{0}	0.3195×10^{0}	0.3067×10^{0}	0.3025×10^{0}
0.4	0.3758×10^{0}	0.3081×10^{0}	0.2585×10^{0}	0.2266×10^{0}	0.2094×10^{0}	0.2040×10^{0}
0.6	0.3269×10^{0}	0.2312×10^{0}	0.1694×10^{0}	0.1355×10^{0}	0.1206×10^{0}	0.1167×10^{0}
0.8	0.2603×10^{0}	0.1415×10^{0}	0.7404×10^{-1}	0.4453×10^{-1}	0.3722×10^{-1}	0.3704×10^{-1}
1.0	0.1787×10^{0}	0.4230×10^{-1}	-0.2635×10^{-1}	-0.4818×10^{-1}	-0.4459×10^{-1}	-0.3932×10^{-1}

When $kd=0.7$,

r/d \ θ (rad.)	0	$\pi/10$	$\pi/5$	$3\pi/10$	$2\pi/5$	$\pi/2$
0.0	0.4262×10^{0}	0.4262×10^{0}	0.4262×10^{0}	0.4262×10^{0}	0.4262×10^{0}	0.4262×10^{0}
0.2	0.4137×10^{0}	0.3718×10^{0}	0.3376×10^{0}	0.3127×10^{0}	0.2978×10^{0}	0.2929×10^{0}
0.4	0.3767×10^{0}	0.2975×10^{0}	0.2395×10^{0}	0.2020×10^{0}	0.1815×10^{0}	0.1752×10^{0}
0.6	0.3166×10^{0}	0.2054×10^{0}	0.1327×10^{0}	0.9149×10^{-1}	0.7225×10^{-1}	0.6697×10^{-1}
0.8	0.2363×10^{0}	0.9936×10^{-1}	0.1860×10^{-1}	-0.2168×10^{-1}	-0.3645×10^{-1}	-0.3929×10^{-1}
1.0	0.1403×10^{0}	-0.1491×10^{-1}	-0.1005×10^{0}	-0.1408×10^{0}	-0.1531×10^{0}	-0.1543×10^{0}

(to be continued)

When $kd=0.8$, (continued)

r/d \ θ (rad.)	0	$\pi/10$	$\pi/5$	$3\pi/10$	$2\pi/5$	$\pi/2$
0.0	0.4331×10^{0}	0.4331×10^{0}	0.4331×10^{0}	0.4331×10^{0}	0.4331×10^{0}	0.4331×10^{0}
0.2	0.4178×10^{0}	0.3695×10^{0}	0.3300×10^{0}	0.3014×10^{0}	0.2842×10^{0}	0.2785×10^{0}
0.4	0.3728×10^{0}	0.2818×10^{0}	0.2149×10^{0}	0.1710×10^{0}	0.1467×10^{0}	0.1390×10^{0}
0.6	0.3007×10^{0}	0.1737×10^{0}	0.8905×10^{-1}	0.3800×10^{-1}	0.1185×10^{-1}	0.4011×10^{-2}
0.8	0.2065×10^{0}	0.5182×10^{-1}	-0.4493×10^{-1}	-0.1024×10^{-1}	-0.1326×10^{0}	-0.1410×10^{0}
1.0	0.9774×10^{-1}	-0.7508×10^{-1}	-0.1827×10^{0}	-0.2555×10^{0}	-0.3056×10^{0}	-0.3256×10^{0}

When $kd=0.9$,

r/d \ θ (rad.)	0	$\pi/10$	$\pi/5$	$3\pi/10$	$2\pi/5$	$\pi/2$
0.0	0.4369×10^{0}	0.4369×10^{0}	0.4369×10^{0}	0.4369×10^{0}	0.4369×10^{0}	0.4369×10^{0}
0.2	0.4184×10^{0}	0.3633×10^{0}	0.3183×10^{0}	0.2856×10^{0}	0.2658×10^{0}	0.2593×10^{0}
0.4	0.3644×10^{0}	0.2611×10^{0}	0.1844×10^{0}	0.1330×10^{0}	0.1036×10^{0}	0.9411×10^{-1}
0.6	0.2795×10^{0}	0.1364×10^{0}	0.3777×10^{-1}	-0.2707×10^{-1}	-0.6478×10^{-1}	-0.7736×10^{-1}
0.8	0.1721×10^{0}	-0.3823×10^{-5}	-0.1167×10^{0}	-0.2018×10^{0}	-0.2623×10^{0}	-0.2864×10^{0}
1.0	0.5309×10^{-1}	-0.1361×10^{0}	-0.2722×10^{0}	-0.3989×10^{0}	-0.5285×10^{0}	-0.5962×10^{0}

When $kd=1.0$,

r/d \ θ (rad.)	0	$\pi/10$	$\pi/5$	$3\pi/10$	$2\pi/5$	$\pi/2$
0.0	0.4372×10^{0}	0.4372×10^{0}	0.4372×10^{0}	0.4372×10^{0}	0.4372×10^{0}	0.4372×10^{0}
0.2	0.4150×10^{0}	0.3525×10^{0}	0.3015×10^{0}	0.2641×10^{0}	0.2414×10^{0}	0.2338×10^{0}
0.4	0.3509×10^{0}	0.2344×10^{0}	0.1466×10^{0}	0.8548×10^{-1}	0.4893×10^{-1}	0.3668×10^{-1}
0.6	0.2529×10^{0}	0.9320×10^{-1}	-0.2265×10^{-1}	-0.1079×10^{0}	-0.1656×10^{0}	-0.1872×10^{0}
0.8	0.1336×10^{0}	-0.5552×10^{-1}	-0.1978×10^{0}	-0.3265×10^{0}	-0.4449×10^{0}	-0.5006×10^{0}
1.0	0.8187×10^{-2}	-0.1962×10^{0}	-0.3685×10^{0}	-0.5784×10^{0}	-0.8540×10^{0}	-0.1014×10^{1}

Table 4. The variation of the amplitudes in the domain D_1. (The coordinates (x, y) used in this table are dimensionless quantities divided by a half width (d) of the canal).

When $kd=0.02$,

y \ x	0.0	0.2	0.4	0.6	0.8	1.0
0.0	1.957	1.957	1.957	1.957	1.957	1.957
−0.2	1.957	1.957	1.957	1.957	1.957	1.957
−0.4	1.957	1.957	1.957	1.957	1.957	1.957
−0.6	1.957	1.957	1.957	1.957	1.957	1.957
−0.8	1.957	1.957	1.957	1.957	1.957	1.957
−1.0	1.957	1.957	1.957	1.957	1.957	1.957

When $kd=0.1$,

y \ x	0.0	0.2	0.4	0.6	0.8	1.0
0.0	1.786	1.786	1.786	1.787	1.787	1.787
−0.2	1.787	1.787	1.787	1.786	1.786	1.786
−0.4	1.787	1.787	1.787	1.786	1.786	1.786
−0.6	1.787	1.787	1.787	1.786	1.786	1.786
−0.8	1.787	1.787	1.787	1.786	1.786	1.786
−1.0	1.787	1.787	1.787	1.786	1.786	1.786

When $kd=0.2$,

y \ x	0.0	0.2	0.4	0.6	0.8	1.0
0.0	1.606	1.606	1.606	1.607	1.608	1.610
−0.2	1.607	1.607	1.607	1.606	1.606	1.606
−0.4	1.607	1.607	1.607	1.606	1.606	1.606
−0.6	1.607	1.607	1.607	1.606	1.606	1.606
−0.8	1.607	1.607	1.607	1.606	1.606	1.606
−1.0	1.607	1.607	1.607	1.606	1.606	1.606

When $kd=0.3$,

y \ x	0.0	0.2	0.4	0.6	0.8	1.0
0.0	1.459	1.459	1.460	1.462	1.465	1.471
−0.2	1.462	1.462	1.462	1.462	1.462	1.462
−0.4	1.463	1.462	1.462	1.461	1.461	1.461
−0.6	1.463	1.463	1.462	1.461	1.461	1.461
−0.8	1.463	1.462	1.462	1.461	1.461	1.461
−1.0	1.462	1.462	1.462	1.461	1.461	1.461

(to be continued)

When $kd=0.4$, (continued)

y \ x	0.0	0.2	0.4	0.6	0.8	1.0
0.0	1.337	1.338	1.340	1.344	1.351	1.362
−0.2	1.342	1.342	1.343	1.343	1.345	1.346
−0.4	1.344	1.344	1.344	1.343	1.342	1.342
−0.6	1.345	1.344	1.344	1.343	1.342	1.342
−0.8	1.344	1.344	1.344	1.343	1.342	1.342
−1.0	1.344	1.344	1.343	1.343	1.342	1.342

When $kd=0.5$,

y \ x	0.0	0.2	0.4	0.6	0.8	1.0
0.0	1.233	1.234	1.237	1.245	1.258	1.277
−0.2	1.241	1.242	1.243	1.245	1.248	1.250
−0.4	1.245	1.245	1.244	1.244	1.243	1.243
−0.6	1.246	1.245	1.244	1.243	1.242	1.242
−0.8	1.246	1.245	1.244	1.243	1.242	1.242
−1.0	1.245	1.245	1.244	1.243	1.243	1.242

When $kd=0.6$,

y \ x	0.0	0.2	0.4	0.6	0.8	1.0
0.0	1.140	1.142	1.148	1.161	1.182	1.211
−0.2	1.154	1.154	1.156	1.160	1.166	1.170
−0.4	1.159	1.159	1.159	1.159	1.159	1.159
−0.6	1.161	1.161	1.160	1.158	1.157	1.157
−0.8	1.161	1.161	1.160	1.158	1.157	1.156
−1.0	1.161	1.160	1.159	1.158	1.157	1.157

When $kd=0.7$,

y \ x	0.0	0.2	0.4	0.6	0.8	1.0
0.0	1.056	1.058	1.068	1.088	1.119	1.163
−0.2	1.075	1.076	1.080	1.087	1.096	1.102
−0.4	1.084	1.084	1.084	1.085	1.086	1.087
−0.6	1.087	1.086	1.085	1.084	1.083	1.082
−0.8	1.087	1.087	1.085	1.084	1.082	1.082
−1.0	1.087	1.086	1.085	1.084	1.082	1.082

(to be continued)

When $kd=0.8$, (continued)

y \ x	0.0	0.2	0.4	0.6	0.8	1.0
0.0	0.977	0.980	0.994	1.024	1.068	1.129
−0.2	1.004	1.005	1.011	1.022	1.037	1.046
−0.4	1.016	1.016	1.017	1.019	1.022	1.023
−0.6	1.021	1.020	1.019	1.018	1.017	1.016
−0.8	1.022	1.021	1.020	1.017	1.016	1.015
−1.0	1.021	1.021	1.019	1.018	1.016	1.015

When $kd=0.9$,

y \ x	0.0	0.2	0.4	0.6	0.8	1.0
0.0	0.901	0.906	0.926	0.966	1.027	1.108
−0.2	0.937	0.939	0.948	0.964	0.986	0.999
−0.4	0.954	0.955	0.957	0.961	0.965	0.968
−0.6	0.961	0.961	0.960	0.958	0.958	0.958
−0.8	0.963	0.962	0.960	0.958	0.956	0.955
−1.0	0.962	0.962	0.960	0.958	0.956	0.955

When $kd=1.0$,

y \ x	0.0	0.2	0.4	0.6	0.8	1.0
0.0	0.826	0.833	0.860	0.914	0.994	1.099
−0.2	0.873	0.877	0.889	0.912	0.943	0.961
−0.4	0.896	0.897	0.901	0.907	0.915	0.919
−0.6	0.906	0.905	0.905	0.904	0.904	0.904
−0.8	0.909	0.908	0.906	0.903	0.901	0.901
−1.0	0.909	0.908	0.906	0.903	0.901	0.900

Table 5. The variation of the phases in the domain D_1
(The coordinates (x, y) used in this table are dimensionless quantities divided by a half width (d) of the canal).

When $kd=0.02$,

y \ x	0.0	0.2	0.4	0.6	0.8	1.0
0.0	0.6270×10^{-1}	0.6249×10^{-1}	0.6173×10^{-1}	0.6039×10^{-1}	0.5870×10^{-1}	0.5675×10^{-1}
−0.2	0.6583×10^{-1}	0.6566×10^{-1}	0.6515×10^{-1}	0.6435×10^{-1}	0.6346×10^{-1}	0.6298×10^{-1}
−0.4	0.6929×10^{-1}	0.6918×10^{-1}	0.6887×10^{-1}	0.6843×10^{-1}	0.6800×10^{-1}	0.6781×10^{-1}
−0.6	0.7298×10^{-1}	0.7292×10^{-1}	0.7274×10^{-1}	0.7250×10^{-1}	0.7228×10^{-1}	0.7220×10^{-1}
−0.8	0.7681×10^{-1}	0.7677×10^{-1}	0.7667×10^{-1}	0.7654×10^{-1}	0.7644×10^{-1}	0.7639×10^{-1}
−1.0	0.8072×10^{-1}	0.8070×10^{-1}	0.8064×10^{-1}	0.8057×10^{-1}	0.8052×10^{-1}	0.8049×10^{-1}

When $kd=0.1$,

y \ x	0.0	0.2	0.4	0.6	0.8	1.0
0.0	0.1967×10^{0}	0.1957×10^{0}	0.1918×10^{0}	0.1850×10^{0}	0.1756×10^{0}	0.1666×10^{0}
−0.2	0.2123×10^{0}	0.2115×10^{0}	0.2089×10^{0}	0.2049×10^{0}	0.2003×10^{0}	0.1979×10^{0}
−0.4	0.2296×10^{0}	0.2291×10^{0}	0.2275×10^{0}	0.2253×10^{0}	0.2231×10^{0}	0.2221×10^{0}
−0.6	0.2481×10^{0}	0.2477×10^{0}	0.2468×10^{0}	0.2456×10^{0}	0.2445×10^{0}	0.2441×10^{0}
−0.8	0.2672×10^{0}	0.2670×10^{0}	0.2665×10^{0}	0.2658×10^{0}	0.2653×10^{0}	0.2651×10^{0}
−1.0	0.2867×10^{0}	0.2866×10^{0}	0.2863×10^{0}	0.2859×10^{0}	0.2857×10^{0}	0.2855×10^{0}

When $kd=0.2$,

y \ x	0.0	0.2	0.4	0.6	0.8	1.0
0.0	0.2875×10^{0}	0.2854×10^{0}	0.2773×10^{0}	0.2632×10^{0}	0.2455×10^{0}	0.2252×10^{0}
−0.2	0.3185×10^{0}	0.3166×10^{0}	0.3112×10^{0}	0.3029×10^{0}	0.2935×10^{0}	0.2885×10^{0}
−0.4	0.3527×10^{0}	0.3516×10^{0}	0.3483×10^{0}	0.3436×10^{0}	0.3391×10^{0}	0.3371×10^{0}
−0.6	0.3895×10^{0}	0.3888×10^{0}	0.3869×10^{0}	0.3844×10^{0}	0.3821×10^{0}	0.3812×10^{0}
−0.8	0.4277×10^{0}	0.4273×10^{0}	0.4263×10^{0}	0.4249×10^{0}	0.4237×10^{0}	0.4233×10^{0}
−1.0	0.4667×10^{0}	0.4665×10^{0}	0.4659×10^{0}	0.4659×10^{0}	0.4646×10^{0}	0.4644×10^{0}

When $kd=0.3$,

y \ x	0.0	0.2	0.4	0.6	0.8	1.0
0.0	0.3412×10^{0}	0.3378×10^{0}	0.3252×10^{0}	0.3031×10^{0}	0.2754×10^{0}	0.2437×10^{0}
−0.2	0.3870×10^{0}	0.3841×10^{0}	0.3756×10^{0}	0.3626×10^{0}	0.3478×10^{0}	0.3399×10^{0}
−0.4	0.4381×10^{0}	0.4362×10^{0}	0.4311×10^{0}	0.4237×10^{0}	0.4166×10^{0}	0.4135×10^{0}
−0.6	0.4929×10^{0}	0.4918×10^{0}	0.4889×10^{0}	0.4849×10^{0}	0.4814×10^{0}	0.4799×10^{0}
−0.8	0.5501×10^{0}	0.5495×10^{0}	0.5478×10^{0}	0.5457×10^{0}	0.5439×10^{0}	0.5432×10^{0}
−1.0	0.6085×10^{0}	0.6082×10^{0}	0.6073×10^{0}	0.6062×10^{0}	0.6052×10^{0}	0.6049×10^{0}

(to be continued)

When $kd=0.4$, (continued)

y \ x	0.0	0.2	0.4	0.6	0.8	1.0
0.0	0.3747×10^{0}	0.3699×10^{0}	0.3521×10^{0}	0.3213×10^{0}	0.2826×10^{0}	0.2387×10^{0}
−0.2	0.4348×10^{0}	0.4308×10^{0}	0.4188×10^{0}	0.4005×10^{0}	0.3797×10^{0}	0.3686×10^{0}
−0.4	0.5024×10^{0}	0.4997×10^{0}	0.4925×10^{0}	0.4821×10^{0}	0.4721×10^{0}	0.4677×10^{0}
−0.6	0.5751×10^{0}	0.5736×10^{0}	0.5694×10^{0}	0.5637×10^{0}	0.5588×10^{0}	0.5567×10^{0}
−0.8	0.6511×10^{0}	0.6502×10^{0}	0.6478×10^{0}	0.6449×10^{0}	0.6424×10^{0}	0.6414×10^{0}
−1.0	0.7288×10^{0}	0.7284×10^{0}	0.7271×10^{0}	0.7255×10^{0}	0.7242×10^{0}	0.7237×10^{0}

When $kd=0.5$,

y \ x	0.0	0.2	0.4	0.6	0.8	1.0
0.0	0.3956×10^{0}	0.3892×10^{0}	0.3657×10^{0}	0.3251×10^{0}	0.2747×10^{0}	0.2181×10^{0}
−0.2	0.4696×10^{0}	0.4642×10^{0}	0.4483×10^{0}	0.4239×10^{0}	0.3966×10^{0}	0.3819×10^{0}
−0.4	0.5531×10^{0}	0.5497×10^{0}	0.5399×10^{0}	0.5261×10^{0}	0.5128×10^{0}	0.5069×10^{0}
−0.6	0.6435×10^{0}	0.6415×10^{0}	0.6358×10^{0}	0.6283×10^{0}	0.6217×10^{0}	0.6190×10^{0}
−0.8	0.7381×10^{0}	0.7369×10^{0}	0.7338×10^{0}	0.7298×10^{0}	0.7264×10^{0}	0.7251×10^{0}
−1.0	0.8351×10^{0}	0.8344×10^{0}	0.8328×10^{0}	0.8307×10^{0}	0.8290×10^{0}	0.8283×10^{0}

When $kd=0.6$,

y \ x	0.0	0.2	0.4	0.6	0.8	1.0
0.0	0.4078×10^{0}	0.3997×10^{0}	0.3698×10^{0}	0.3185×10^{0}	0.2556×10^{0}	0.1863×10^{0}
−0.2	0.4953×10^{0}	0.4884×10^{0}	0.4681×10^{0}	0.4369×10^{0}	0.4022×10^{0}	0.3836×10^{0}
−0.4	0.5944×10^{0}	0.5899×10^{0}	0.5774×10^{0}	0.5596×10^{0}	0.5425×10^{0}	0.5350×10^{0}
−0.6	0.7020×10^{0}	0.6994×10^{0}	0.6921×10^{0}	0.6824×10^{0}	0.6739×10^{0}	0.6704×10^{0}
−0.8	0.8149×10^{0}	0.8135×10^{0}	0.8095×10^{0}	0.8044×10^{0}	0.8000×10^{0}	0.7983×10^{0}
−1.0	0.9311×10^{0}	0.9303×10^{0}	0.9282×10^{0}	0.9255×10^{0}	0.9233×10^{0}	0.9224×10^{0}

When $kd=0.7$,

y \ x	0.0	0.2	0.4	0.6	0.8	1.0
0.0	0.4136×10^{0}	0.4035×10^{0}	0.3665×10^{0}	0.3036×10^{0}	0.2279×10^{0}	0.1463×10^{0}
−0.2	0.5142×10^{0}	0.5055×10^{0}	0.4801×10^{0}	0.4415×10^{0}	0.3986×10^{0}	0.3758×10^{0}
−0.4	0.6284×10^{0}	0.6227×10^{0}	0.6070×10^{0}	0.5846×10^{0}	0.5632×10^{0}	0.5539×10^{0}
−0.6	0.7529×10^{0}	0.7496×10^{0}	0.7405×10^{0}	0.7282×10^{0}	0.7174×10^{0}	0.7130×10^{0}
−0.8	0.8840×10^{0}	0.8822×10^{0}	0.8772×10^{0}	0.8707×10^{0}	0.8562×10^{0}	0.8630×10^{0}
−1.0	0.1019×10^{1}	0.1018×10^{1}	0.1015×10^{1}	0.1012×10^{1}	0.1009×10^{1}	0.1008×10^{1}

(to be continued)

When $kd=0.8$, (continued)

y \ x	0.0	0.2	0.4	0.6	0.8	1.0
0.0	0.4145×10^{0}	0.4021×10^{0}	0.3571×10^{0}	0.2818×10^{0}	0.1934×10^{0}	0.1011×10^{0}
−0.2	0.5278×10^{0}	0.5171×10^{0}	0.4859×10^{0}	0.4389×10^{0}	0.3874×10^{0}	0.3602×10^{0}
−0.4	0.6567×10^{0}	0.6497×10^{0}	0.6302×10^{0}	0.6026×10^{0}	0.5763×10^{0}	0.5648×10^{0}
−0.6	0.7977×10^{0}	0.7935×10^{0}	0.7822×10^{0}	0.7670×10^{0}	0.7535×10^{0}	0.7481×10^{0}
−0.8	0.9467×10^{0}	0.9444×10^{0}	0.9381×10^{0}	0.9300×10^{0}	0.9231×10^{0}	0.9204×10^{0}
−1.0	0.1100×10^{1}	0.1099×10^{1}	0.1096×10^{1}	0.1092×10^{1}	0.1088×10^{1}	0.1087×10^{1}

When $kd=0.9$,

y \ x	0.0	0.2	0.4	0.6	0.8	1.0
0.0	0.4111×10^{0}	0.3961×10^{0}	0.3423×10^{0}	0.2541×10^{0}	0.1538×10^{0}	0.5313×10^{1}
−0.2	0.5372×10^{0}	0.5241×10^{0}	0.4865×10^{0}	0.4302×10^{0}	0.3694×10^{0}	0.3377×10^{0}
−0.4	0.6804×10^{0}	0.6719×10^{0}	0.6479×10^{0}	0.6144×10^{0}	0.5824×10^{0}	0.5686×10^{0}
−0.6	0.8375×10^{0}	0.8324×10^{0}	0.8183×10^{0}	0.7995×10^{0}	0.7829×10^{0}	0.7762×10^{0}
−0.8	0.1004×10^{1}	0.1001×10^{1}	0.9933×10^{0}	0.9832×10^{0}	0.9747×10^{0}	0.9713×10^{0}
−1.0	0.1176×10^{1}	0.1174×10^{1}	0.1171×10^{1}	0.1165×10^{1}	0.1161×10^{1}	0.1159×10^{1}

When $kd=1.0$,

y \ x	0.0	0.2	0.4	0.6	0.8	1.0
0.0	0.4041×10^{0}	0.3862×10^{0}	0.3226×10^{0}	0.2213×10^{0}	0.1108×10^{0}	0.5066×10^{-2}
−0.2	0.5433×10^{0}	0.5276×10^{0}	0.4825×10^{0}	0.4161×10^{0}	0.3458×10^{0}	0.3098×10^{0}
−0.4	0.7005×10^{0}	0.6901×10^{0}	0.6611×10^{0}	0.6206×10^{0}	0.5824×10^{0}	0.5659×10^{0}
−0.6	0.8732×10^{0}	0.8669×10^{0}	0.8496×10^{0}	0.8266×10^{0}	0.8063×10^{0}	0.7981×10^{0}
−0.8	0.1056×10^{1}	0.1053×10^{1}	0.1043×10^{1}	0.1031×10^{1}	0.1021×10^{1}	0.1016×10^{1}
−1.0	0.1247×10^{1}	0.1245×10^{1}	0.1240×10^{1}	0.1233×10^{1}	0.1228×10^{1}	0.1226×10^{1}

31. 河口近傍における長波について [II]

地震研究所　桃　井　高　夫

筆者はすでに河口近傍における長波に関する研究をベッセル函数の線型近似の範囲でおこなつた．そしてその近似を第2次近似まで上げて解析をおこなつた結果をまとめたのが今回の報告である．その結果，第1近似ではわからなかつた河口近傍の波の細かい変化が判明してきた．新しくわかつたことは次のようなことである．

河口近くの水路の中には，波の回折によつて生じたと思われる丘陵部ができる．

水路への進入波は最初，広海 (open sea) より河口の中心に向つて進み (波の峰線は三角形状をなしている)，中心に向うにつれてこれらの波は水路の軸方向に向きを変えてゆく．

近似が第1近似より第2近似 (本報告の) に進むにつれて，広海における減衰反射波はあまり変化を受けず，多少これらの波の指向性が失われるだけである．

本報告の理論の展開に用いられた基本原理は筆者によつて展開された buffer domain の方法である．